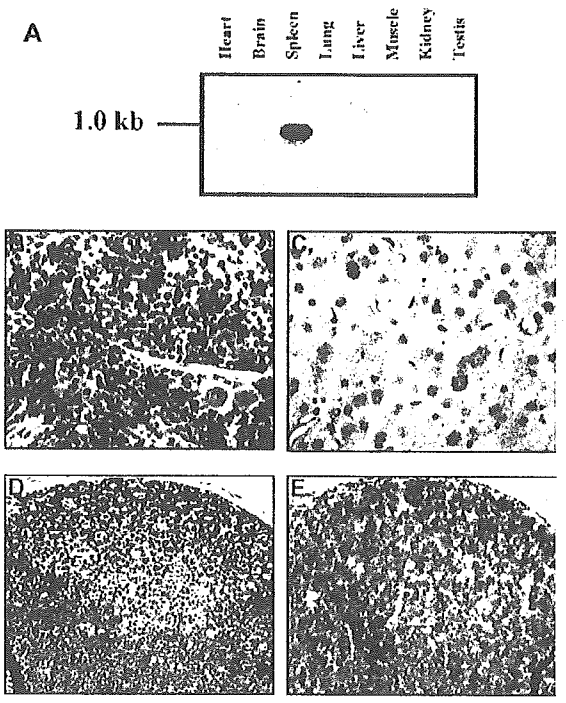

Figure 4. Murine HTm4 expression patterns in the adult mouse. (A) Northern analysis of HTm4 transcript distribution in adult mouse. Adult mouse multiple tissue Northern blot was probed with 32P labeled full length HTm4 cDNA. Of the tissue RNA extracts present on this membrane, only the spleen sample displayed significant hybridization. Visualized band corresponds to the approximately 1 kb murine HTm4 transcript. This commercial blot has been normalized to beta-actin by the manufacturer (BD Biosciences, CLONTECH, Palo Alto, CA). (B–E). Immunohistohemical staining of adult murine spleen, brain and lymph node for murine HTm4. Representative sections of formalin-fixed paraffin embedded adult murine spleen, lymph node, or brain were stained with anti-murine HTm4 antibody as described in Methods. Positive cytoplasmic staining of cells (DAB chromogen with hematoxylin counterstain) was restricted to either hematopoietic cells within the red pulp of the spleen (B; 400× original magnification) or neurons of the cerebral cortex of the adult murine brain (C; 400× original magnification). Germinal center B-lymphocytes within secondary lymphoid follicles also express murine HTm4 (D; 200× original magnification). The pattern of expression is identical to that of the murine HTm4 interacting protein KAP (E; 200× original magnification). (F) Flow cytometric analysis of HTm4 expression in cell populations derived from adult murine bone marrow. Mouse bone marrow cells were isolated as described in Methods. Aliquots of cells were co-stained with either control rabbit IgG or anti-murine HTm4 and antibodies to specific surface markers for various bone marrow subpopulations. Cell-type specific co-stains were as follows: B-lymphocytes (CD19), T-lymphocytes (CD3), monocytes (CD11b), nucleated red blood cells (Ter119), and granulocytes (GR-1).

by the manufacturer (Caltag Laboratories Inc., Burlingame, CA, USA). Cells were labeled with 2 μg/ml of polyclonal anti-murine HTm4 for 20 min, followed by the incubation with anti-rabbit IgG-FITC (Fab) (Caltag, Burlingame, CA), along with CD19-PE (BD Pharmingen, San Diego, CA), CD3-PE (BD Pharmingen), Ter119 (BD Pharmingen), Gr1-PE (BD Pharmingen) and CD11b-PE (Caltag). The flow cytometry analyses were performed on a FACScan flow cytometer (Becton Dickinson Immunocytometry Systems, San Diego, CA). In the control group, bone marrow cells were labeled with 2 μg/ml of Rabbit IgG (Sigma, St. Louis, MO) for 20 min, followed by the incubation with anti-rabbit IgG-FITC (Fab) (Caltag).

Results

cDNA, genomic and protein sequence of murine HTm4

Our database analysis identified a murine expressed sequence tag (EST) that was highly homologous to the human *HTm4* cDNA sequence. This enabled the design of a specific PCR primer that was used to isolate a clone from a murine cDNA library. After several rounds of RACE-PCR and DNA sequence analysis, we obtained a single contiguous cDNA corresponding to murine *HTm4*. The cDNA and translated protein sequence of murine HTm4 was deposited in Gene Bank (accession number AY184359).

Murine HTm4 is a 213 amino acid protein with a predicted molecular weight of approximately 25 kDa. Proscan analysis reveals that murine HTm4 has no obvious enzymatic or protein–protein interaction domains, but does contain a single consensus sequence for *N*-glycosylation. Human HTm4 is similarly devoid of amino acid sequence clues to its functional role, and also contains a single *N*-glycosylation site and a PKC substrate motif.

We compared the protein sequences of murine HTm4 and human HTm4 using ClustalW alignment (Oxford Molecular and MacVector, Accelrys, San Diego, CA). Across the ~220 amino acid sequence, 119 identities (55%) and 27 functional similarities (12%) were found. Murine HTm4, like its human counterpart, has four putative transmembrane domains resulting in very similar predicted structures (Figure 1). Both murine HTm4 and human HTm4 proteins can be defined as members of the MS4A protein family, on the basis of their four-transmembrane structure and sequence homology. Murine HTm4 is designated MS4A3.

We have previously assigned the chromosomal location of human *HTm4* to 11q13.1 (Donato *et al.* 2002). Location of the murine gene for *HTm4* was assigned using genomic BLAST against the available mouse genome (NCBI BLAST facility). Probes were murine *HTm4* genomic sequence and human *HTm4* cDNA sequence, which gave identical results. Using this analysis, the murine *HTm4* gene was localized to chromosome 19A. We note that the murine *HTm4* gene is clustered in this location with the *MS4A2* gene, corresponding to the mouse *FcεRIβ* subunit and the gene for *MS4A6D*. This cluster is highly reminiscent of that

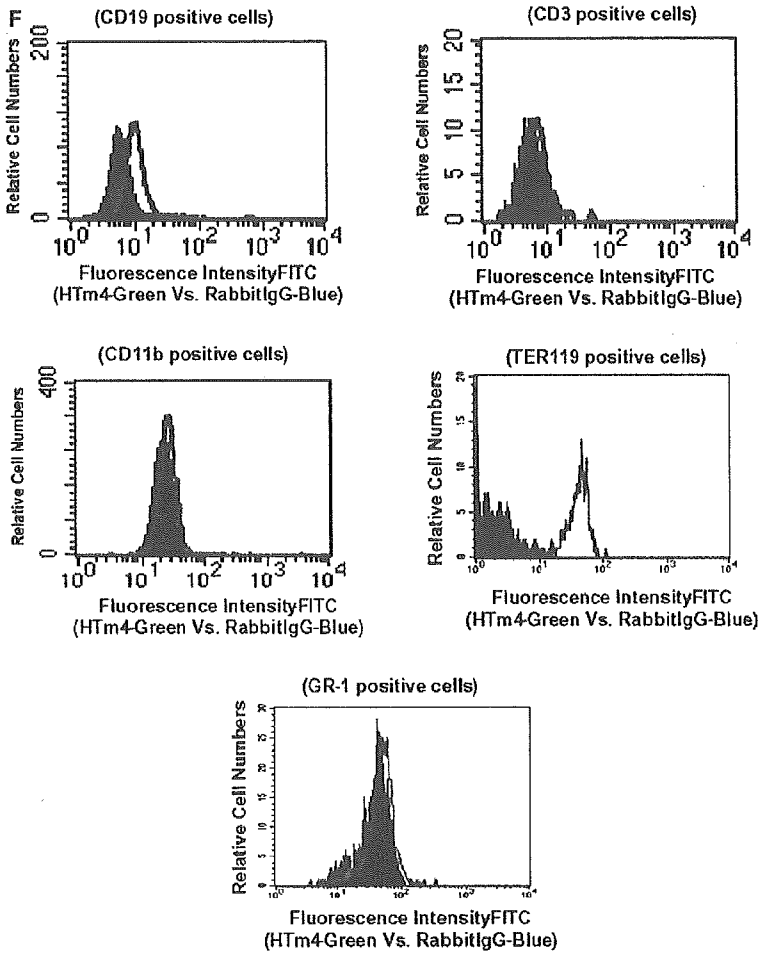

Figure 4. (Continued).

located in humans at chromosome 11q13.1, which has been linked to atopic/allergic disorders (Adra *et al.* 1999). Other members of the MS4A family are located at more distal locations also on the mouse chromosome 19, including *MS4A10, MS4A8 and MS4A7* (Ishibashi *et al.* 2001, Liang *et al.* 2001, Liang and Tedder, 2001).

Further analysis of the murine genomic sequence revealed that the murine *HTm4* gene has the same six-intron and seven-exon gene structure as the human HTm4 gene (Figure 2A). In addition, the full length of murine *HTm4* gene (Gene Bank accession number AY258288) spans approximately 11 kb, which is also comparable to the human *HTm4* gene (Adra et al., 1999). Sequence analysis up to 1 kb upstream from the ATG (Figure 2B) showed that the putative promoter region contains many potential binding sites for transcription factors that are involved in hematopoiesis, immune response and cell proliferation, such as AP1 (Mathas *et al.* 2002), CEBPB (Akira *et al.* 1990), IK1-2 (Georgopoulos *et al.* 1994) and GATA1-3 (Tsai *et al.* 1994, Pandolfi *et al.* 1995, McDevitt *et al.* 1997).

Murine HTm4 expression pattern in developing mouse embryos reveals restriction to hematopoietic and neural tissues

One of the most notable features of the human HTm4 protein is its relatively restricted tissue expression pattern. Current data suggest that human HTm4 is expressed, in adult tissues, in cells of the hematopoietic lineage. In our characterization of murine HTm4, we asked if this tissue specificity is also a feature of the mouse system. We first probed Northern blots for the presence of murine *HTm4* transcripts in RNA extracts from whole murine embryos at defined stages of development (Figure 3A). Sufficient levels of a ~1.0 kb murine HTm4 transcript are present for detection by at least day 13 and continue to be expressed at day 17. Northern analysis provides a valuable, but low-resolution, picture of the expression levels of a given transcript during development. In order to localize expression of murine HTm4 within specific tissuetypes, we performed immunohistochemistry on tissue from various embryonic stages. Initially, we validated the

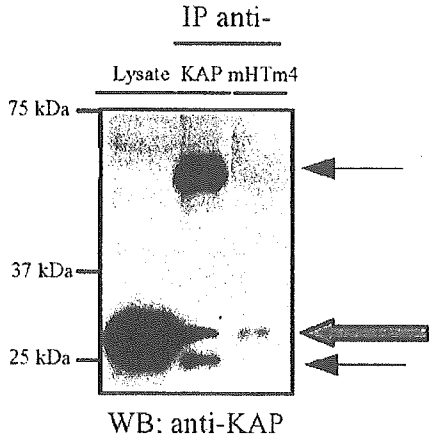

Figure 5. Co-immunoprecipitation of HTm4 and KAP proteins in murine leukocytes. P815 mouse mast cells (10^7 cells per lane) were lysed as described in Methods. Total protein precipitates (lysate) were produced by acetone precipitation or immunoprecipitation was performed using either 2 μg/lane anti-KAP (mouse monoclonal) or 11 μg/lane anti-murine HTm4 (rabbit polyclonal). Samples were resolved by 10% SDS-PAGE and visualized using anti-KAP western blot. KAP appears as a 32 kDa band in lysate from these cell (open arrow). KAP is also present in anti-KAP and anti-murine HTm4 immunocomplexes. Filled arrows mark presence of antibody heavy (55 kDa) and light (26 kDa) chains in immunoprecipitations using mouse anti-KAP and visualized with the same antibody.

specificity of our anti-murine HTm4 antibody raised against the N-terminal amino acids 4-19 via western blot. Figure 3B shows that our anti-murine HTm4 antibody specifically recognizes a 25-kDa protein from adult murine spleen cells (right lane). Importantly, anti-murine HTm4 also recognizes the amino-terminus of murine HTm4 when expressed as a glutathione *S*-transferase fusion protein (Figure 3B, left lane). A carboxy-terminal murine HTm4 fusion protein is not recognized (center lane). These data confirm the specificity of the antiserum for the amino-terminus of murine HTm4.

Immunohistochemical analysis was performed for murine HTm4 expression in formalin-fixed, paraffin-embedded day 8–16 embryonic murine tissues. As anticipated, hematopoietic expression was confirmed in murine development. We observed that from embryonic days (E) 8–10, murine HTm4 expression appears in small numbers of hematopoietic cells resident in blood islands and vessels (Figure 3C top left panel and inset). By E12–13, murine HTm4 expression is seen within the hematopoietic cells now resident in the liver, where mononuclear cells show positive staining (Figure 3D). Morphologically, these cells are compatible with both erythroid and myeloid precursors, with some staining also noted in megakaryocytes. At E14, expression persists in the liver hematopoietic cells and appears in splenic red pulp hematopoietic cells for the first time (data not shown). Staining was not present within non-germinal center B-cells of the spleen. Scattered cortical thymocyte staining was also noted, later in development (E15–16) (data not shown).

In addition to staining of murine embryonic hematopoietic cells, embryos from E8 through 16 stained with murine HTm4 show a developmental pattern of expression in the central nervous system (CNS) (Figure 3E–L). In general, murine HTm4 is expressed only in regions outside the ventricular zone, suggesting upregulation as cells begin to differentiate (Figure 3F–K). Specifically, at E8 and E9, the CNS is negative. By E10, however, expression is visible at the periphery of the neural tube (i.e., away from the ventricular zone neuropithelium) at all levels. Sagittal sections at E11–12 show expression that is somewhat stronger, particularly within the dorsal prosencephalon, mesencephalon, isthmal plate, cerebellar plate, and pontine plate, and along the ventral aspect of the spinal cord. Faint expression of murine HTm4 is noted in the trigeminal and paravertebral ganglia. At E12, faint expression appears in the anterior prosencephalon, and at E13, additional positivity is noted in the neocortex rostrally, the diencephalon ventral to the neuroepithelium, and along the peripheral (subpial) regions caudally, corresponding to dorsal and ventral gray matter columns. At this stage, the peripheral nerve roots are now faintly positive. At E14, sagittal sections demonstrate strong immunoreactivity in the ventral telencephalon and diencephalon, tegmentum of the mesencephalon, anterior and posterior pons, medulla, and ventral spinal cord, but absence of staining in the ventricular zone neuroepithelium. There is also staining in the peripheral nerves and paravertebral ganglia (Figure 3L). The tectum and the eye are negative. E15 sagittal sections show staining as in the E14 embryo, additionally with faint staining in the pretectum and dorsal root ganglia, and in the ganglion cell layer of the retina (Figure 3E). The ependyma of the fourth ventricle and the myenteric plexus of the gut are also positive. E16 sagittal sections additionally revealed staining in the olfactory bulb (a structure not identified in earlier age sections). To determine whether the HTm4-expressing cells were undifferentiated neural progenitor cells, serial sections were stained for nestin at E12 and E16 (Figure 3M and N). In these sections, nestin highlights ventricular zone neuroepithelial cells and radial (possibly glial) cell processes, but do not stain the presumed differentiating cells in the primitive neocortex and ventral diencephalon (at E12 and E16), the caudoputamen, anterior and posterior pontine nuclear groups, superior tectal neuroepithelium, superior central raphe and reticular formation of the midbrain and pons, or the subventricular zone (at E16) that are positive on HTm4 immunostaining (Figure 3F–K) Thus, an apparently non-overlapping pattern of expression is noted with these two antibodies. For all ages studied, appropriate negative controls (sections incubated with preimmune serum and/or

peptide, or with the secondary antibody only) showed no staining.

Murine HTm4 is expressed in cells of the hematopoietic lineage and brain in adult mouse

We analyzed the expression pattern of murine *HTm4* mRNA in adult animals using Northern blot. Assaying multiple tissues revealed that of the tissue RNA preparations probed in this experiment, only the spleen extract contained sufficient RNA for detection with the murine *HTm4* probe (Figure 4A). Transcript size of approximately 1 kb is consistent with the human *HTm4* mRNA. We also performed a dot blot analysis on adult mouse tissues and observed a similar degree of restriction in *HTm4* expression pattern (data not shown).

Immunohistochemical analysis of adult murine tissues yielded similar patterns to that seen in developing embryos. Strong cytoplasmic staining for murine HTm4 was noted within maturing hematopoietic cells of the spleen (Figure 4B) and in lymphoid cells (presumably B-lymphocytes) within germinal centers of lymphoid tissue of lymph nodes (Figure 4D) and Peyer's patches of the gut (not shown). As was previously demonstrated in human lymphoid tissue (Donato *et al.* 2002), murine HTm4 co-localized within germinal centers with mKAP protein (Figure 4E), a putative functional regulator of HTm4 activity. Additionally, in adult murine brain, murine HTm4 expression is identified in cells morphologically consistent with neurons in the hypothalamus, thalamus, cerebral cortex (Figure 4C), and, more faintly, in the hippocampus.

To further characterize the specific lineages of hematopoietic cells expressing murine HTm4, we isolated cells from murine bone marrow and spleen and assessed their expression of intracellular murine HTm4 by flow cytometry. Staining patterns from isolated hematopoietic cells were identical in both tissues. Representative data from bone marrow studies is shown in Figure 4F. Murine HTm4 expression was noted in Ter119 positive erythroid precursors and a smaller fraction of CD19-positive B-lymphocytes. Minimal murine HTm4 detection was observed in GR-1 positive granulocytic forms, CD11b-positive monocytic elements, or CD3 positive T-lymphocytes.

Association of murine HTm4 with the KAP phosphatase

In the human, we have proposed that HTm4 is involved in cell cycle regulation in hematopoietic cells, based on the association between HTm4 and the KAP phosphatase (Hannon *et al.* 1994, Poon & Hunter 1995) in human hematopoietic cells (Donato *et al.* 2002). In murine germinal centers, the cell populations that express murine HTm4 and KAP co-localize as assessed by immunohistochemical staining for these proteins (Figure 4D and E), raising the possibility that these proteins may be functionally associated. We asked if murine HTm4 is also physically associated with KAP. We identified a murine leukocytic line, P815, with expression of murine HTm4 and KAP. Co-immunoprecipitation using the P815 cell line demonstrates that immunocomplexes isolated using either anti-KAP or anti-murine HTm4 antibodies contain KAP protein (Figure 5). These data indicate that in the murine system, as in human cells, murine HTm4 and KAP form a physiological complex.

Discussion

In this study, we asked whether the cell cycle-associated protein HTm4, previously characterized by us in the adult human (Adra *et al.* 1994; Adra *et al.* 1999, Donato *et al.* 2002; Nakajima *et al.* 2004), shared similar structural, biochemical and functional features, in the developing and adult mouse. To that end, we undertook the cloning, genomic organization, and expression analysis of murine HTm4, and demonstrated its interaction with a protein known to interact with the human homologue of HTm4.

In our previous work, we cloned the human *HTm4* gene and assigned two key features to the protein. First, the expression of human HTm4 appears largely restricted to the hematopoietic cell lineages (Adra *et al.*, 1994). Second, a function for human HTm4 as an adapter protein that contributes to cell cycle progression was supported (Donato *et al.* 2002). Murine HTm4 is highly similar to human HTm4 at the DNA and amino acid level, and both proteins display a similar predicted four-transmembrane structure (Figure 1). Comparison to two reported HTm4 cDNA sequences (Hulett *et al.* 2001; Liang *et al.* 2001) revealed two amino acid sense variants (Ser162Ala and Ser211Thr). CLUSTAL alignment analysis and chromosomal grouping places murine *HTm4*, like human *HTm4*, in the MS4 protein superfamily (Hulett *et al.* 2001, Ishibashi *et al.* 2001, Liang *et al.* 2001, Liang & Tedder 2001). A similar genomic structure between the two genes is also identified with both genes containing a six-intron and seven-extron arrangement. Several promoter regions for transcription factors important for hematopoiesis, immune response and cell proliferation, such as AP1, CEBPB, IK1-2, and GATA1-3 are also identified. The presence of the GATA promoter regions is particularly interesting given the critical role of these transcription factors in erythopoiesis (Tsai *et al.* 1994, Pandolfi *et al.* 1995, McDevitt *et al.* 1997). The high level of expression of murine HTm4 in erythroid progenitors suggests GATA-regulated transcriptional regulation of HTm4 and a potential role for HTm4 in erythroid differentiation. Additionally, GATA-3 appears to be critical for neural development

as well (Pandolfi *et al.* 1995). Overall, we have found a high degree of conservation of structure and function of this gene and its protein across species, suggesting a fundamentally conserved biological function.

In addition to similarities at the genomic and protein level, the tissue expression pattern of murine HTm4 also has similarities to that seen in the human. Immunohistochemical techniques reveal expression of murine HTm4 within early hematopoietic cells of the blood islands starting at E8. Hematopoietic cell expression persists as hematopoiesis moves to the liver then spleen later in embryonic life. Immunohistochemical analysis of adult murine tissues confirms that murine HTm4 appears to continue to be largely hematopoietically restricted. Clusters of predominantly mononuclear cells present within the spleen react with antibody directed against murine HTm4. These cells morphologically appear most consistent with nucleated erythroid, myeloid and lymphoid elements. To confirm this morphologic impression and define more specifically the hematopoietic cell lineages expressing murine HTm4, multicolor flow cytometric analysis was performed on permeabilized, disaggregated spleen and bone marrow cells. These studies reveal that the majority of Ter119-expressing nucleated erythroid precursors display positive staining for murine HTm4. Very weak expression was noted within cells co-expressing the myeloid markers GR-1 and CD11b by flow cytometry. In addition, murine HTm4 co-expression was also noted in CD19-positive B-lymphocytes within the marrow. Further evidence for expression in the B-lymphoid population comes from the strong immunoreactivity for murine HTm4 antibody in germinal center B-cells in lymph nodes and Peyer's patches. The predominance of staining in germinal center cells as opposed to surrounding mantle or marginal zone cells suggests an upregulation of murine HTm4 during the germinal center reaction. Minimal staining was seen in the T-lymphoid cell population by immunohistochemistry or flow cytometry.

In contrast to previous human studies in which analysis of expression was restricted to mature tissues, the current work includes extensive study of both embryonic and adult murine tissues. Examination of the developing mouse has expanded the tissue distribution of expression from being solely hematopoietic, as in adult human tissues, to include prominent expression in the developing and mature murine nervous system, a novel and unexpected finding. By E10, immunohistochemical staining can detect murine HTm4 expression within cells that are morphologically consistent with differentiating neuronal and glial cells of the developing central nervous system, and by E15–16, prominent expression is seen as well in the peripheral nervous system. Importantly, there is no overlap in the expression of murine HTm4, most highly expressed in more mature neuronal and glial cells, and nestin, a protein that is associated with primitive neural cells. The strong expression of murine HTm4, and non-overlapping pattern of expression with nestin, in the developing brain suggests a role of murine HTm4 in CNS development and neural cell differentiation. Once a site expresses HTm4, it appears to retain expression into adulthood. Further analysis of the specific role of murine HTm4 expression in CNS cells is needed. These data also suggest that a CNS-based phenotype, in addition to an effect on hematopoiesis, may be a feature of experimental murine HTm4 deficient mice.

Our previous work on human HTm4 has suggested that this is an intracellular protein. Unlike several other MS4 family members (Tedder *et al.* 1988, Ravetch & Kinet, 1991), HTm4 is not present on the cell surface, but rather resides in the perinuclear compartment within the ER/Golgi apparatus. We have shown that human HTm4 is part of a complex containing the KAP phosphatase (Donato *et al.* 2002). Immunoprecipitation studies and western blotting confirm a similar biochemical association between murine HTm4 and KAP protein in a murine leukocyte cell line, P815, suggesting that murine HTm4 plays a similar role in mouse and human leukocytes. Although we have already detected HTm4 expression in primary human mast cells, basophils, eosinophils (Adra *et al.* 1994, Nakajima *et al.* 2004), and also in murine P815, another group did not detect HTm4 mRNA in P815 by PCR (Hulett *et al.* 2001). This could be due to a very low copy number of mRNA that nevertheless corresponds to a very high level or protein. It is also possible that HTm4 mRNA may not have been detectable in their experiments. We have not yet been able to conduct similar studies on CNS cells that express murine HTm4, and thus we do not know if murine HTm4 in the embryonic CNS cells also physically interacts with KAP. Interestingly, preliminary data (not shown) using immunohistochemical staining suggest that murine HTm4 and KAP may co-localize in developing CNS, but proof of this interaction will require co-purification from dissociated embryonic CNS cells.

In summary, we have examined the distribution of murine HTm4 in murine tissues. Murine HTm4 distribution in adult mice closely resembles the highly restricted pattern seen in adult human tissues. In studying the murine embryo, we have revealed a potentially exciting facet of HTm4 biology and function, namely, the strong expression in the developing CNS, and apparent persistence in a subset of adult neural cells. Other aspects of HTm4 biology are closely parallelled between murine and human systems. In hematopoietic cells from both systems, HTm4 binds with KAP and therefore, likely functions as a component of the cell cycle machinery. These data will aid in the creation and analysis of a murine HTm4 deficient

mouse in an attempt to address the role of HTm4 in both hematopoietic and CNS development. In addition, further analysis of the protein interactions and cell-cycle regulatory capability of HTm4 will identify its importance in both contexts.

Acknowledgements

This work was supported by NIH Grant AI 43663 from the National Institute of Allergy and Infectious Diseases and by Grant RSG-01-241-01-LIB from the American Cancer Society (to C. Adra). Histological and immunohistochemical services were provided by the DF/HCC cancer center Hematopathology core lab supported by NIH-P30CA6516; NIH-HL44851, NIH-HL65909, and the Richard Saltonstall Charitable Foundation (to D.T. Scadden). This work was also supported by the Adra family and is dedicated to the memories of Dr. Ramzi Cotran and Dr. Stephen H. Robinson. We would like to acknowledge the technical assistance of Ms. Vuong Nguyen.

References

Adra CN, Lelias JM, Kobayashi H, Kaghad M, Morrison P, Rowley JD, Lim B (1994) Cloning of the cDNA for a hematopoietic cell-specific protein related to CD20 and the beta subunit of the high-affinity IgE receptor: evidence for a family of proteins with four membrane-spanning regions. *Proc Natl Acad Sci USA*, **91**: 10178–10152.

Adra CN, Manor D, Ko JL, Zhu S, Horiuchi T, Van Aelst L, Cerione RA, Lim B (1997) RhoGDIgamma: a GDP-dissociation inhibitor for Rho proteins with preferential expression in brain and pancreas. *Proc Natl Acad Sci USA*, **94**: 4279–4284.

Adra CN, Mao XQ, Kawada H, Gao PS, Korzycka B, Donate JL, Shaldon SR, Coull P, Dubowitz M, Enomoto T, Ozawa A, Syed SA, Horiuchi T, Khaeraja R, Khan R, Lin SR, Flinter F, Beales P, Hagihara A, Inoko H, Shirakawa, T, Hopkin JM (1999) Chromosome 11q13 and atopic asthma. *Clin Genet* **55**: 431–437.

Akira S, Isshiki H, Sugita T, Tanabe O, Kinoshita S, Nishio Y, Nakajima T, Hirano T, Kishimoto T (1990) A nuclear factor for IL-6 expression (NF-IL6) is a member of a C/EBP family. *Embo J* **9**: 1897–1906.

Barnhill JC, Stokes AJ, Koblan-Huberson M, Shimoda LM, Muraguchi A, Adra CN, Turner H (2004) RGA protein associates with a TRPV ion channel during biosynthesis and trafficking. *J Cell Biochem* **91**: 808–820.

Collee JM, ten Kate LP, de Vries HG, Kliphuis JW, Bouman K, Scheffer, H, Gerritsen J (1993) Allele sharing on chromosome 11q13 in sibs with asthma and atopy. *Lancet* **342**: 936.

Donato JL, Ko J, Kutok JL, Cheng T, Shirakawa T, Mao XQ, Beach D, Scadden DT, Sayegh MH, Adra CN (2002) Human HTm4 is a hematopoietic cell cycle regulator. *J Clin Invest*, **109**: 51–58.

Folster-Holst R, Moises HW, Yang L, Fritsch W, Weissenbach J, Christophers E (1998) Linkage between atopy and the IgE high-affinity receptor gene at 11q13 in atopic dermatitis families. *Hum Genet*, **102**: 236–239.

Georgopoulos K, Bigby M, Wang JH, Molnar A, Wu P, Winandy S, Sharpe A (1994) The Ikaros gene is required for the development of all lymphoid lineages. *Cell*, **79**: 143–156.

Hannon GJ, Casso D, Beach D (1994) KAP: a dual specificity phosphatase that interacts with cyclin- dependent kinases. *Proc Natl Acad Sci USA* **91**: 1731–1735.

Hulett MD, Pagler E, Hornby JR (2001) Cloning and characterization of a mouse homologue of the human haematopoietic cell-specific four-transmembrane gene HTm4. *Immunol Cell Biol*, **79**: 345–349.

Ishibashi K, Suzuki M, Sasaki S, Imai M (2001) Identification of a new multigene four-transmembrane family (MS4A) related to CD20, HTm4 and beta subunit of the high-affinity IgE receptor. *Gene*, **264**: 87–93.

Kyte J, Doolittle RF (1982) A simple method for displaying the hydropathic character of a protein. *J Mol Biol* **157**: 105–132.

Liang Y, Buckley TR, Tu L, Langdon SD, Tedder TF (2001) Structural organization of the human MS4A gene cluster on Chromosome 11q12. *Immunogenetics*, **53**: 357–368.

Liang, Y, Tedder TF (2001) Identification of a CD20-, Fcepsilon-RIbeta-, and HTm4-related gene family: sixteen new MS4A family members expressed in human and mouse. *Genomics* **72**: 119–127.

Mathas S, Hinz M, Anagnostopoulos I, Krappmann D, Lietz A, Jundt F, Bommert K, Mechta-Grigoriou F, Stein H, Dorken, B, Scheidereit C (2002) Aberrantly expressed c-Jun and JunB are a hallmark of Hodgkin lymphoma cells, stimulate proliferation and synergize with NF-kappa B. *Embo J* **21**: 4104–4113.

McDevitt MA, Shivdasani RA, Fujiwara Y, Yang H, Orkin SH (1997) A 'knockdown' mutation created by cis-element gene targeting reveals the dependence of erythroid cell maturation on the level of transcription factor GATA-1. *Proc Natl Acad Sci USA*, **94**: 6781–6785.

Mitaku S, Suzuki K, Odashima S, Ikuta K, Suwa M, Kukita F, Ishikawa, M, Itoh H (1995) Interaction stabilizing tertiary structure of bacteriorhodopsin studied by denaturation experiments. *Proteins*, **22**: 350–362.

Nakajima T, Iikura M, Okayama Y, Matsumoto K, Uchiyama C, Shirakawa T, Yang X, Adra CN, Hirai K, Saito H (2004) Identification of granulocyte subtype-selective receptors and ion channels by using a high-density oligonucleotide probe array. *J Allergy Clin Immunol*, **113**: 528–535.

Pandolfi PP, Roth ME, Karis A, Leonard MW, Dzierzak E, Grosveld FG, Engel JD, Lindenbaum MH (1995) Targeted disruption of the GATA3 gene causes severe abnormalities in the nervous system and in fetal liver haematopoiesis. *Nat Genet* **11**: 40–44.

Poon RY, Hunter T (1995) Dephosphorylation of Cdk2 Thr160 by the cyclin-dependent kinase- interacting phosphatase KAP in the absence of cyclin. *Science* **270**: 90–93.

Quandt, K, Frech, K, Karas, H, Wingender, E, Werner I (1995) Mat Ind and Mat Inspector: new fast and versatile tools for detection of consensus matches in nucleotide sequence data. *Nuclear Acids Res* **23**: 4878–4884.

Ra C, Jouvin MH, Kinet JP (1989) Complete structure of the mouse mast cell receptor for IgE (Fc epsilon RI) and surface expression of chimeric receptors (rat-mouse-human) on transfected cells. *J Biol Chem* **264**: 15323–15327.

Ravetch JV, Kinet JP (1991) Fc receptors. *Annu Rev Immunol* **9**: 457–492.

Shirakawa T, Hashimoto T, Furuyama J, Takeshita, T, Morimoto K (1994) Linkage between severe atopy and chromosome 11q13 in Japanese families. *Clin Genet* **46**: 228–232.

Tedder TF, Streuli M, Schlossman SF, Saito H (1988) Isolation and structure of a cDNA encoding the B1 (CD20) cell-surface antigen of human B lymphocytes. *Proc Natl Acad Sci USA*, **85**: 208–212.

Tsai FY, Keller G, Kuo FC, Weiss M, Chen J, Rosenblatt M, Alt FW, Orkin SH (1994) An early haematopoietic defect in mice lacking the transcription factor GATA-2. *Nature* **371**: 221–226.

van Herwerden L, Harrap SB, Wong ZY, Abramson MJ, Kutin JJ, Forbes AB, Raven J, Lanigan, A, Walters EH (1995) Linkage of high-affinity IgE receptor gene with bronchial hyperreactivity, even in absence of atopy. *Lancet* **346**: 1262–1265.

Biosci. Biotechnol. Biochem., **69** (3), 638–641, 2005

Note

Molecular Monitoring of the Developmental Bacterial Community in the Gastrointestinal Tract of Japanese Infants

Prapa SONGJINDA,[1] Jiro NAKAYAMA,[1,†] Yumiko KUROKI,[1] Shigemitsu TANAKA,[1] Sanae FUKUDA,[2] Chikako KIYOHARA,[3] Tetsuro YAMAMOTO,[2,4] Kunio IZUCHI,[5] Taro SHIRAKAWA,[2] and Kenji SONOMOTO[1]

[1]*Laboratory of Microbial Technology, Division of Microbial Science and Technology, Department of Bioscience and Biotechnology, Faculty of Agriculture, Graduate School, Kyushu University, 6-10-1 Hakozaki, Higashi-ku, Fukuoka 812-8581, Japan*

[2]*Department of Health Promotion and Human Behavior, Kyoto University Graduate School of Public Health, Yoshida-Konoe cho, Sakyo-ku, Kyoto 606-8501, Japan*

[3]*Department of Preventive Medicine, Division of Social Medicine, Graduate School of Medical Sciences, Kyushu University, Maidashi 3-1-1, Higashi-ku, Fukuoka 812-8582, Japan*

[4]*Total Technology Consultant, 1-20-2 Ebisunishi, Shibuya-ku, Tokyo 150-0021, Japan*

[5]*Izuchi Hospital, 4-15-6 Yakuin, Chuo-ku, Fukuoka 810-0022, Japan*

Received October 18, 2004; Accepted November 26, 2004

The dynamics of the developmental bacterial community in the Japanese neonatal gastrointestinal tract were examined by monitoring 16S ribosomal RNA gene (rDNA) diversity in fecal samples by PCR and denaturing gradient gel electrophoresis (DGGE). The results showed a certain pattern common in infants without antibiotic treatment, in which aerobes, *e.g.*, *Pseudomonas*, appeared first and were then immediately replaced by facultative anaerobe, *Enterococcus*, *Streptococcus*, and *Enterobacteriaceae* through the first month, and finally strictly anaerobic *Bifidobactrerium* appeared.

Key words: denaturing gradient gel electrophoresis (DGGE); gastrointestinal tract; infant; 16S rRNA; intestinal microbiota

Soon after birth, bacterial colonization starts in the previously germfree gastrointestinal tract and commensal host-microbial relationships begin.[1,2] The colonizing bacteria contribute to maintenance of the mucosal barrier, facilitate carbohydrate assimilation, and modulate the mucosal immune system. Thus, the initial development of intestinal microbiota is considered to have great influence on the health of the infant. In this study, the succession of the gastrointestinal bacterial community was examined for the first two months in nine Japanese infants by monitoring 16S ribosomal RNA gene (rDNA) diversity in fecal samples.

All infant subjects (infants nos. 1, 2, 5, 6, 10, 20, 24, 25, and 33) participated in this study were vaginally delivered. Infant no. 5 was fed formula milk and the other infants were fed both breast and formula milk during the sampling period. Infants no. 1 and no. 33 were subjected to antibiotic therapy, receiving cefalex (50 mg/kg, 4 times a day) the first four days, whereas infant no. 5 was treated on day 0 only. Fecal samples were collected on day 0/1, day 3, day 5, month 1, and month 2 (there was no month-2 sample from infant no. 5). All the parents of our subjects gave written informed consent and the Ethics Committee of the Faculty of Medicine of Kyoto University approved this study protocol.

DNA was isolated from each fecal sample using a bead beating method essentially as previously described,[3] except for 2–3 times washing of the fecal sample before the bead beating step. In order to construct 16S rDNA libraries, a V1–V3 region of 16S rDNA was amplified from each sample by PCR with 8UA (5′-AGAGTTTGATCCTGGCTCAG-3′)[4] and 519B (5′-ATTACCGCSGCTGCTG-3′)[5] primers, and cloned into a pGEM-T vector (Promega, Madison, WI), and transformed in *E. coli* JM109. About ten clones from each library were sequenced. In total, 357 clones were sequenced and the ribotypes found are summarized with the result of the database search in Table 1.

PCR-denaturing gradient gel electrophoresis (PCR-DGGE), which allowed rapid and efficient molecular fingerprinting of gut microbiota,[3,6] was performed in order to monitor the succession of the infant fecal bacterial community. The variable region V2–V3 of 16S rDNA was amplified by PCR using primers HDA1-GC (5′-CGC CCG GGG CGC GCC CCG GGC GGG GCG

† To whom correspondence should be addressed. Tel/Fax: +81-92-642-3020; E-mail: nakayama@agr.kyushu-u.ac.jp

Table 1. List of Ribotypes Obtained in This Study

Ribotype	Closest sequence relative[a] (species)	% identity	Numbers			Accession no.
			clones	subjects	DGGE[b]	
Gram-positive facultative anaerobes						
Ef	*Enterococcus faecalis*	99.4	25	4	7	AY635946
Ss	*Streptococcus salivarius*	99.8	14	6	3	AY635947
Sp	*Streptococcus parasanguis*	96.4	12	3	7	AY635948
Se	*Staphylococcus epidermidis*	100.0	11	4	8	AY635949
Pa	*Propionibacterium avidum*	99.0	4	3	0	AY635950
Em	*Enterococcus faecium*	99.8	4	2	6	AY635951
Sa	*Streptococcus anginosus*	99.8	4	1	1	AY635952
Lg	*Lactobacillus gasseri*	99.8	2	2	0	AY635953
St	*Streptococcus thermophilus*	99.8	2	1	5	AY635954
Sm'	*Streptococcus mitis*	96.6	2	1	0	AY635955
Sm	*Streptococcus mitis*	99.0	1	1	4	AY635956
Sc	*Streptococcus cremoris*	99.1	1	1	3	AY635957
Si	*Streptococcus infantarius*	99.6	1	1	1	AY635958
Gram-positive strict anaerobes						
Cb	*Clostridium butyricum*	100.0	25	4	4	AY635959
Bd	*Bifidobacterium dentium*	99.0	11	5	5	AY635960
Bp	*Bifidobacterium pseudocatanulatum*	100.0	11	2	5	AY635961
Fm	*Finegoldia magna*	98.8	2	2	0	AY635962
Rm	*Ruminococcus* sp.	99.0	2	1	1	AY635963
Ch	*Clostridium hathewayi*	98.6	3	1	1	AY635964
Gram-positive aerobes						
Mm	*Micrococcus mucilaginosus*	98.8	5	2	1	AY635965
Ar	*Acinetobacter rhizospaerae*	98.7	5	1	0	AY635966
Gram-negative facultative anaerobes						
Es	*Enterobacter* sp. B901-2	99.8	32	5	6	AY635967
Kp	*Klebsiella pneumoniae*	99.2	31	6	2	AY635968
Km	*Klebsiella milletis*	99.0	19	8	6	AY635969
Ec	*Escherichia coli*	99.2	15	2	3	AY635970
Ko	*Klebsiella oxytoca*	99.6	12	2	2	AY635971
Cd	*Citrobacter diversus*	98.5	5	2	0	AY635972
Kr	*Klebsiella rennanqify*	99.0	9	3	4	AY635973
Cg	*Calymmatobacterium granulomatis*	99.0	7	4	1	AY635974
Ea	*Enterobacter aerogenes*	97.8	5	2	0	AY635975
Km'	*Klebsiella milletis*	99.0	3	3	1	AY635976
Sf	*Escherichia coli*	99.4	3	2	0	AY635977
Ko'	*Klebsiella oxytoca*	98.3	2	1	1	AY635978
Kr'	*Klebsiella rennanqify*	98.9	2	1	0	AY635979
Gram-negative strict anaerobes						
Bu	*Bacteroides uniformis*	99.4	8	3	1	AY635980
Vp	*Veillonella parvula*	98.9	1	1	1	AY635981
Vp'	*Veillonella parvula*	98.4	1	1	1	AY635982
Gram-negative aerobes						
Pm	*Pseudomonas marginalis/reactans/veronii*	99.4	28	5	5	AY635983
Fh	*Flavobacterium heparinum*	98.1	8	3	3	AY635984
Pt	*Pseudomonas tolaasii*	99.6	7	4	2	AY635985
Ad	*Acidovorax deflvii*	99.4	6	1	1	AY635986
Ph	*Phyllobacterium myrsinacearum*	99.6	4	1	0	AY635987
Pr	*Pseudomonas trivialis/poae*	99.6	2	2	2	AY635988

Ribotypes found with more than two clones in the 16S rDNA libraries or found only once but also detected in DGGE are listed.
[a]Cultured bacteria in Genbank showing highest identity as a result of Blast search.
[b]The number of bands corresponding to the indicated species in the DGGE (Fig. 1).

GGG GCA CGG GGG GAC TCC TAC GGG AGG CAG CAG T-3′) and HDA2 (5′-GTA TTA CCG CGG CTG CTG GCA C-3′).[7] The PCR condition was as follows: 94 °C for 5 min, 30 cycles consisting of 94 °C for 40 s, 58 °C for 20 s, and 72 °C for 1 min, and finally 72 °C for 5 min. DGGE analysis was performed as described by Muyzer *et al.*[8] and Heilig *et al.*[9] using a Dcode System apparatus (Bio-Rad, CA). Each band in the DGGE gel was assigned one of the ribotypes in Table 1 either by sequencing of DNA fragments excised from the DGGE gel or by comparing band positions with those of reference clones derived from the 16S rDNA clone library.

Figure 1 shows the DGGE profile of nine subjects. Although each subject showed individual banding patterns, a stepwise development from aerobic to

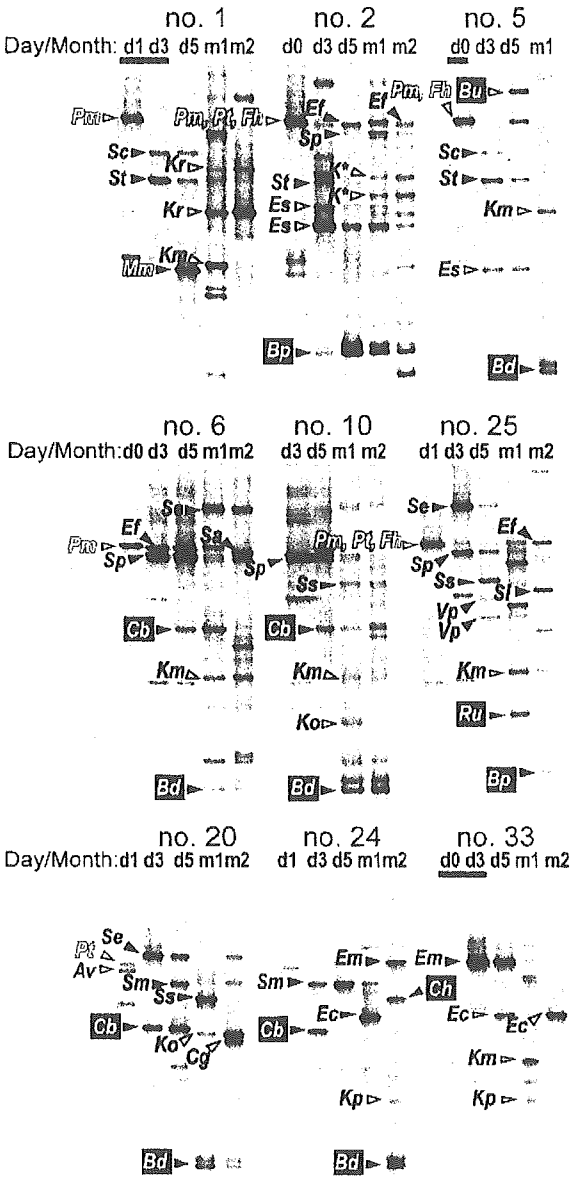

Fig. 1. PCR-DGGE Profiles Representing the Fecal Bacterial Community in the First Two Months of Nine Infants.

The bands identified with ribotypes in the 16S rDNA clone libraries are indicated by arrowheads with their names listed in Table 1, except K* which indicates unidentified *Klebsiella* spp. Open and black arrowheads represent Gram-negative and Gram-positive bacteria respectively. Open, black, and outlined letters represent aerobic, facultatively anaerobic, and strictly anaerobic bacteria respectively. Bold lines under the sampling days indicate the period of antibiotic treatment. Electrophoresis was done in 8% polyacylamide gel with a denaturing gradient of 30–65%, where 100% corresponds to 7 M urea and 40% formamide. The gel was run at 100 V for 6.5 h at 60 °C and then stained in 1 × SYBR Gold (Molecular Probes, Eugene, OR).

anaerobic microbial ecosystem was observed in the succession of bacterial composition in the seven subjects (nos. 2, 5, 6, 10, 20, 24, and 25) without successive antibiotic treatment in the first four days. In the beginning, bands corresponding to aerobic Gram-negative bacteria such as *Pseudomonas* appeared and they were then replaced by facultatively anaerobic bacteria such as *Streptococcus*, *Enterococcus*, or *Staphylococcus epidermidis* and *Enterobacteriaceae*. Particularly, strong bands closely related to *Streptococcus parasanguis*, *Streptococcus cremoris* and *Streptococcus thermophilus* appeared on day 3 in many subjects. It is interesting to note that a large majority of the bacteria types such as *Streptococcus parasanguis*, *Streptococcus mitis*, *Streptococcus salivarius*, *Bifidobacterium dentium*, and *Veillonella parvula* detected in this period are regarded as oral-origin bacteria rather than intestinal species. This suggests that these oral-origin bacteria may transiently colonize the intestine during this period.

Bifidobacteria detected in the bottom part of the DGGE gel appeared within two months in most subjects. In infant no. 2, *Bifidobacterium pseudocatanulatum* colonized predominantly from day 3 and continued until 2 months of age. This subject was only the case which agreed with the finding of previous studies,[6,10,11] showing that bifidobacteria usually appear and become dominant within a week after birth. The appearance of bifidobacterial bands in infant no. 2 was concomitant with a decrease in *Enterobacteriaceae* bands, which appeared as dominant on day 3. A concomitant decrease in *Enterobacteriaceae* with an increase of bifidobacteria in breast-milk fed infants has been reported.[12] Bands related to *Clostridium butyricum* were also detected in infants nos. 6, 10, 20, and 24, in which they appeared earlier than bifidobacteria. The other strict anaerobes, *Veillonella parvula*-like bacteria, and *Ruminococcus* sp. were found only in infant no. 25. *Bacteroides uniformis* was detected only at day 5 in infant no. 5 (antibiotic treatment on day 0) who was the only subject brought up only on formula milk.

Infants nos. 1 and 33 treated with antibiotics in the first 3 days showed relatively simple microbiota, and the developmental patterns deviated remarkably from the trends observed in the other subjects without antibiotic treatment. In infant no. 1, a dominant band corresponding to *Micrococcus mucilaginosus*, which is not a common inhabitant of the intestine, appeared suddenly on day 5 and completely disappeared during month 1. In infant no. 33, a dominant band corresponding to *Enterococcus faecium* appeared on day 3 and disappeared during month 1. No bands corresponding to bifidobacteria and other strict anaerobes were found in the testing period in either baby and only bands corresponding to *Enterobacteriaceae* were found during month 1 and month 2, suggesting domination by *Enterobacteriaceae*. This was also indicated by the data of random sequencing of 16S rDNA clone libraries, which showed that all 30 clones sequenced from the month-1 and month-2 libraries of these two subjects belonged to *Enterobacteriaceae*. These data showed that antibiotic treatment at the beginning of life has strong

influence on the establishment of a normal microbial ecosystem in the intestine.

In conclusion, this molecular study indicates the stepwise development from aerobic to anaerobic microbial ecosystem with a variety of bacterial groups, although the process differed among individuals at the species level. The step of the bacterial colonization in the gastrointestinal tract is most likely a key to the developmental process. Strong antibiotic treatment interrupted the development of normal microbiota, including bifidobacteria. Further studies with modern molecular methods are needed for understanding of the environmental and host factors affecting the developmental process of neonatal microbiota.

Acknowledgment

We thank all the families who provided fecal samples for this study. This research was supported in part by a Research Grant for Immunology, Allergy, and Organ Transplants from the Ministry of Health and Welfare of Japan, by a grant from Danon Institute for the Promotion of Health and Nutrition, and by a grant from Takeda Science Foundation.

References

1) Mackie, R. I., Sghir, A., and Gaskins, H. R., Developmental microbial ecology of the neonatal gastrointestinal tract. *Am. J. Clin. Nutr.*, **69** (Suppl.), 1035S–1045S (1999).
2) Hooper, L. V., and Gordon, J. I., Commensal host-bacterial relationships in the gut. *Science*, **292**, 1115–1118 (2001).
3) Zoetendal, E. G., Akkermans, A. D. L., and de Vos, W. M., Temperature gradient gel electrophoresis analysis of 16S rRNA from human fecal samples reveals stable and host-specific communities of active bacteria. *Appl. Environ. Microbiol.*, **64**, 3854–3859 (1998).
4) Acinas, S. G., Anton, J., and Rodrigues-Valera, F., Diversity of free-living and attached bacteria in offshore western Mediterranean waters as depicted by analysis of genes encoding 16S rRNA. *Appl. Environ. Microbiol.*, **65**, 514–522 (1999).
5) Bertilsson, S., Cavanaugh, C. M., and Polz, M. F., Sequencing-independent method to generate oligonucleotide probes targeting a variable region in bacterial 16S rRNA by PCR with detachable primers. *Appl. Environ. Microbiol.*, **68**, 6077–6086 (2002).
6) Favier, C. F., Vaughan, E. E., de Vos, W. M., and Akkermans, A. D. L., Molecular monitoring of succession of bacterial communities in human neonates. *Appl. Environ. Microbiol.*, **68**, 219–226 (2002).
7) Tannock, G. W., Munro, K., Harmsen, H. J. M., Welling, G. W., Smart, J., and Gopal, P. K., Analysis of the fecal microflora of human subjects consuming a probiotic product containing *Lactobacillus rhamnosus* DR20. *Appl. Environ. Microbiol.*, **66**, 2578–2588 (2000).
8) Muyzer, G., de Vaal, E., and Uitterlinden, A., Profiling of complex microbial populations by denaturing gel electrophoresis analysis of polymerase chain reaction-amplified genes coding for 16S rRNA. *Appl. Environ. Microbiol.*, **59**, 695–700 (1993).
9) Heilig, H. G. H. J., Zoetendal, E. G., Vaughan, E. E., Marteau, P., Akkermans, A. D. L., and de Vos, W. M., Molecular diversity of *Lactobacillus* spp. and other lactic acid bacteria in the human intestine as determined by specific amplification of 16S ribosomal DNA. *Appl. Environ. Microbiol.*, **68**, 114–123 (2002).
10) Benno, Y., and Mitsuoka, T., Development of intestinal microflora in humans and animals. *Bifidobacteria Microflora*, **5**, 13–25 (1986).
11) Weiling, G. W., Wildeboer-Veloo, L., Raangs, G. C., Franks, A. H., Jansen, G. J., Tonk, R. H. J., Degener, J. E., and Harmsen, H. J. M., Variations of bacterial populations in human feces measured by FISH with group-sepcific 16S rRNA-targeted oligonucleotide probes. In "Molecular Ecological Detection and Identification of Intestinal Microflora", ed. Mitsuoka, T., Japan Scientific Societies Press, Tokyo, pp. 7–18 (2000).
12) Yoshioka, H., Iseki, K., and Fugita, K., Development and differences of intestinal flora in the neonatal period in breast-fed and bottle-fed infants. *Pediatrics*, **72**, 317–321 (1983).

Hum Genet (2005) 117: 16–26
DOI 10.1007/s00439-005-1285-0

ORIGINAL INVESTIGATION

**Mitsuteru Akahoshi · Kazuhiko Obara
Tomomitsu Hirota · Akira Matsuda · Koichi Hasegawa
Naomi Takahashi · Makiko Shimizu
Kazuko Nakashima · Lei Cheng · Satoru Doi
Hiroshi Fujiwara · Akihiko Miyatake · Kimie Fujita
Noritaka Higashi · Masami Taniguchi · Tadao Enomoto
Xiao-Quan Mao · Hitoshi Nakashima · Chaker N. Adra
Yusuke Nakamura · Mayumi Tamari · Taro Shirakawa**

Functional promoter polymorphism in the *TBX21* gene associated with aspirin-induced asthma

Received: 25 November 2004 / Accepted: 25 January 2005 / Published online: 2 April 2005

Abstract Asthma is a phenotypically heterogeneous disorder with many etiologic factors and clinical characteristics. T-bet, a Th1-specific transcription factor of T-box family, has been found to control interferon-γ (IFN-γ) expression in T cells. Mice lacking the T-bet gene (*tbx21*) demonstrate multiple physiological and inflammatory features reminiscent of human asthma. In order to examine whether polymorphisms in the candidate gene, *TBX21*, located on chromosome 17q21.32, are related to the risk of human asthma phenotypes, we have searched for genetic variations in the human *TBX21* gene and identified 24 single nucleotide polymorphisms (SNPs), including five novel SNPs, by direct sequencing in Japanese subjects. Among asthma phenotypes, a promoter −1993T → C SNP, which is in linkage disequilibrium with a synonymous coding 390A → G SNP in exon 1, is significantly associated with a risk of aspirin-induced asthma (AIA; $P=0.004$, $P_c=0.016$). This association has also been confirmed in additional independent samples of asthma with nasal polyposis ($P=0.008$), regardless of aspirin hypersensitivity. Furthermore, our data indicate that the −1993T → C substitution increases the affinity of a particular nuclear protein to the binding site of *TBX21* covering the −1993 position, resulting in increased transcriptional activity of the *TBX21* gene. Thus, in addition to the antigen-driven excess Th2 response, increased T-bet (and subsequent IFN-γ)

M. Akahoshi · K. Obara · T. Hirota · A. Matsuda · N. Takahashi
M. Shimizu · K. Nakashima · M. Tamari (✉) · T. Shirakawa
Laboratory for Genetics of Allergic Diseases,
SNP Research Center, RIKEN Yokohama Institute,
Institute of Physical and Chemical Research (RIKEN),
1-7-22 Suehiro-cho, Tsurumi-ku, Yokohama,
Kanagawa, 230-0045, Japan
E-mail: tamari@src.riken.jp
Tel.: +81-45-5039616
Fax: +81-45-5039615

M. Akahoshi · H. Nakashima
Department of Medicine and Biosystemic Science,
Graduate School of Medical Sciences,
Kyushu University, Fukuoka, Japan

K. Obara
Hitachi Chemical, Tokyo, Japan

K. Hasegawa · K. Nakashima · L. Cheng
X.-Q. Mao · T. Shirakawa
Department of Health Promotion and Human Behavior,
Kyoto University Graduate School of Public Health,
Kyoto, Japan

S. Doi · H. Fujiwara
Osaka Prefectural Medical Center for Respiratory
and Allergic Diseases, Osaka, Japan

A. Miyatake
Miyatake Asthma Clinic,
Osaka, Japan

K. Fujita
College of Nursing,
University of Shiga, Shiga, Japan

N. Higashi · M. Taniguchi
Clinical Research Center,
Sagamihara National Hospital,
Kanagawa, Japan

T. Enomoto
Department of Otolaryngology,
Japanese Red Cross Society,
Wakayama Medical Center, Wakayama, Japan

C. N. Adra
Department of Medicine,
Beth Israel Deaconess Medical Center,
Boston, USA

Y. Nakamura
Laboratory of Molecular Medicine,
Human Genome Center,
Institute of Medical Science,
University of Tokyo, Tokyo, Japan

production in human airways of individuals with the −1993T → C polymorphism could contribute to the development of certain asthma-related phenotypes, such as AIA.

Introduction

Asthma is defined as a chronic inflammatory lung disease that is characterized by airway hyperreactivity, eosinophil inflammation, and mucus hypersecretion resulting in intermittent airway obstruction (Busse and Lemanske 2001). A considerable increase has been noted in the incidence of allergic diseases including asthma in industrialized societies over the past three decades (Bach 2002; Woolcock and Peat 1997). The etiology of asthma is complex and multifactorial; development of the disease is controlled by both host genetic factors and a variety of environmental exposures. Although environmental influences, particularly a decrease in infections because of improved hygiene, might have increased allergic diseases, at least a dozen polymorphic genes have been calculated to regulate asthma, by controlling the inflammatory response, immunoglobulin E (IgE), cytokine, and chemokine production, and airway remodeling (Cookson 1999; Fahy et al. 2000; Umetsu et al. 2002).

Asthma is thought to arise from an imbalance in T helper type 1 (Th1)-Th2 immune regulation, resulting in the driving of the development of Th2-biased immune responses and the overproduction of cytokines such as interleukin 4 (IL-4), IL-5, IL-9, and IL-13, which mediate allergic inflammation (Renauld 2001; Umetsu et al. 2002). In contrast, Th1-type cytokine interferon-γ (IFN-γ) is essential for macrophage activation in cellular defense mechanisms, and IFN-γ-producing Th1 cells have been suggested to protect against allergic responses by dampening the activity of Th2 effector cells (Renauld 2001). However, the evidence from other in vivo studies of asthma conflicts with this hypothesis, suggesting a contribution of IFN-γ to asthmatic airway inflammation (Busse and Lemanske 2001; Salvi et al. 2001).

T-bet is a member of the T-box family of transcription factors that has been found to be expressed in IFN-γ-producing Th1, but not in Th2, cells. T-bet is a transcriptional regulator essential for the lineage commitment of Th1 cells by directly activating Th1-associated genetic programs and repressing Th2 cytokine production (Szabo et al. 2000). Recently, evidence has shown decreased numbers of $CD4^+$ T cells expressing T-bet in the airways of patients with allergic asthma, relative to control subjects (Finotto et al. 2002). Furthermore, deletion of the T-bet gene, *tbx21*, in mice results in airway eosinophilia, Th2 cytokine production, airway hyperresponsiveness (AHR), and changes of airway remodeling without allergen sensitization and challenge. Thus, T-bet-deficient mice demonstrate multiple physiological and inflammatory features reminiscent of human asthma (Finotto et al. 2002).

The human T-bet gene (*TBX21*) is located on chromosome 17q21.32, a region near to that linked with asthma in a genome screen for asthma and skin tests (Dizier et al. 2000; Zhang et al. 1999). Moreover, the region on mouse chromosome 11 that is syntenic to human chromosome 17q12-q22 has been linked to AHR (Zhang et al. 1999). So far, to our knowledge, there have been no reports showing disease-related polymorphism(s) in the *TBX21* gene. Based on these observations, we propose that genetic polymorphism contributes to susceptibility to human asthma and/or related phenotypes. To test this hypothesis, we have searched for polymorphisms in *TBX21* and then conducted a genetic association study in the Japanese population. Finally, we have investigated the functional consequences of disease-related polymorphisms.

Materials and methods

Subjects

We recruited 361 patients with childhood asthma (mean age 9.7 years, range 4–15 years, mean total serum IgE level, 1021 U/ml; 92% of whom were atopic), 313 adult patients with atopic asthma (mean age 49 years, range 20–81 years; mean total IgE, 775.7 U/ml), and 88 adult patients with non-atopic asthma (mean age 59 years, range 42–75 years; mean total IgE, 174.8 U/ml) from the Osaka Prefectural Habikino Hospital and the Miyatake Asthma Clinic. Patients with aspirin-induced asthma (AIA; mean age 53 years, range 24–73 years; 54% of whom were atopic; ≥50% had nasal polyposis) were recruited from the National Sagamihara Hospital. All patients with asthma were diagnosed according to the criteria of the National Institutes of Health, with minor modifications (National Heart, Lung, and Blood Institute, National Institutes of Health, 1997, http://www.nhlbi.nih.gov/guidelines/asthma/asthgdln.htm). The diagnosis of atopic asthma was based on the positive immunoassay test to common allergens (at least one of the following: *Dermatophagoides pteronyssinus*, *Dermatophagoides farinae*, and *Aspergillus fumigatus*) or a higher total serum IgE of ≥400 kU/l, as used in our previous study (Mao et al. 1996). The criteria for a diagnosis of non-atopic asthma was a total serum IgE of <400 kU/l and the absence of allergen-specific IgE (≤ 0.35 kU/l). All patients with AIA were documented to have histories of asthmatic attacks, such as severe bronchoconstriction and nasal symptoms, following the ingestion of more than two different kinds of non-steroidal anti-inflammatory drugs (NSAIDs) or to have had a positive reaction to aspirin systemic challenge. Of 72 AIA patients (58%), 42 were diagnosed on the basis of the aspirin challenge test, as previously described (Kawagishi et al. 2002; Mita et al. 2001). We also

independently recruited 42 asthmatic patients with nasal polyposis (AS/NP; mean age 54 years, range 23–75 years; 73% of whom were atopic). The NP was diagnosed on the basis of history, including nasal symptoms, clinical examination, nasal endoscopy, and sinus computerized tomography scanning. All adult asthmatics, except AIA patients, had no past history of aspirin hypersensitivity. Controls were 640 randomly selected healthy individuals with an age range 18–83 years from the same geographic areas who had neither respiratory symptoms nor history of asthma-related diseases and aspirin hypersensitivity. All subjects in this study were ethnically Japanese and gave written informed consent to participate in the study (or, for individuals less than 16 years old, their parents gave consent), according to the process approved by the Ethical Committee at the SNP Research Center, The Institute of Physical and Chemical Research (RIKEN), Yokohama.

Screening for polymorphisms and genotyping

To identify single-nucleotide polymorphisms (SNPs) in the human *TBX21* gene, we sequenced all six exons, including a minimum of 200 bases of flanking intronic sequence, 2.2 kb of the 5′ flanking region, and 2.5 kb continuous to the 3′ flanking region of the sixth exon from 24 asthmatic subjects (12 unrelated children and 12 adults). Eighteen primer sets were designed on the basis of the *TBX21* genomic sequence from the GenBank database (accession number AC003665; Table 1). For each polymerase chain reaction (PCR), 5 ng genomic DNA was amplified in a total reaction volume of 10 μl containing 12.5 pmol each primer, 3.9 mM $MgCl_2$, 1.25 mM each dNTP, 0.5 U *Taq* polymerase. Cycling conditions were an initial 95°C for 2 min, followed by 37 cycles at 94°C for 30 s, 58°C or 60°C for 30 s, and 72°C for 3 min, with a final extension of 7 min at 72°C. Each fragment amplified by PCR was sequenced by using the BigDye Terminator (Applied Biosystems, Foster City, Calif., USA) on an ABI Prism 3700 Genetic Analyzer (Applied Biosystems). The sequences were analyzed, and polymorphisms were identified by using the SEQUENCHER program (Gene Codes Corporation, Ann Arbor, Mich., USA). Four selected SNPs, viz., −1993T → C, 99C → G, 1298T → C, and 7725T → C, were genotyped by three methods: PCR-RFLP (PCR-restriction fragment lenght polymorphism; for −1993T → C and 1298T → C), Invader assay (for 99C → G), and direct sequencing (for 7725T → C). For PCR-RFLP analysis, we used mismatched primers for the −1993T → C SNP (5′-GGTCTTACTGAAAGCTCTCA-3′ and 5′- TCTCCTCCCCAACACCTTACGC-3′) and for the 1298T → C SNP (5′-GGCTAGTGCAGTAAAGCTTG-3′ and 5′-GGTTTTCACTGGACCAGCCGC-3′) where the changed nucleotides are underlined. The amplified products were digested with *Hha*I (−1993T → C) or *BstU*I (1298T → C) restriction enzymes (New England Biolabs, Bevery, Mass., USA) according to the manufacturer's instructions and were separated by electrophoresis on 4% agarose gels. Based on information available from the public JSNP database (http://snp.ims.u-tokyo.ac.jp), we generated the 99C → G SNP (IMS-JST000934) genotypes by using the Invader assay as previously described (Ohnishi et al. 2001). For the 7725T → C SNP, we performed direct sequencing with primers 5′-TTATCCAGGGTCATAGGGTAG-3′ and 5′-CCTCAGCCTTTAGAGAAGTTG-3′.

Luciferase assay

We generated luciferase reporter constructs, pGL3/−1993T and pGL3/−1993C, by cloning three concatenated copies of a 20-bp fragment of the *TBX21* gene into pGL3-Basic vector (Promega, Madison, Wis., USA) in the *Nhe*I site. The 20-bp primer sets carrying −1993T or −1993C alleles were 5′- CTAGCGGAGAAATGGTGGGTAAGGT T-3′ (forward) and 3′- GCCTCTTTACCACCCATTCCA AGATC-5′ (reverse) or 5′- CTAGC

Table 1 Primer sequences used in screening for SNPs of the human *TBX21* gene

F1	5′-TTTCCAGTAATAGCCGCTCCT-3′	R1	5′-CACAGCCTAGACACTGGTTC-3′
F2	5′-TTGCATAGTTACCATCCACCG-3′	R2	5′-GACCTTGGGATCCTTCACTAC-3′
F3	5′-AAGACTCCATTTGATCTTCAAC-3′	R3	5′-TTCACTCCACAAGGTGTCATG-3′
F4	5′-GTCAGGCTGGGACAGAAATG-3′	R4	5′-TGAGTTGGCTGCATCTTGTAG-3′
F5	5′-CTGGCTGCTGCTGATGCAG-3′	R5	5′-TGTCACTAGAGTCGCAGCGC-3′
F6	5′-AGTACTCGCCAAGAGCGTAG-3′	R6	5′-AAAAACAGACGAGACGTTCTTG-3′
F7	5′-TCGCGCTCAACAACCACCTG-3′	R7	5′-CTCAAAGTAAGACCGGAAAGG-3′
F8	5′-GGCTAGTGCAGTAAAGCTTG-3′	R8	5′-GACCAGAAGCTTGGGCTGTG-3′
F9	5′-CTCTGTTGTGTGGTCAGGAG −3′	R9	5′-TGAGAAGGTATGGAGGTAACC-3′
F10	5′-TTGAAGGAGGCAGTGGCTC-3′	R10	5′-AACACAGCTACCCAAAGTTATC-3′
F11	5′-TTATCCAGGGTCATAGGGTAG-3′	R11	5′-CCTCAGCCTTTAGAGAAGTTG-3′
F12	5′-TAACTTCCTCTACTTTTCCTGG-3′	R12	5′-AAACATCCTGTAGTGGCTGG-3′
F13	5′-TGCCTGGGCACTGTTGCAG-3′	R13	5′-GAAAAACGAACCTTCCTTCCTG-3′
F14	5′-CAACAATGTGACCCAGGTAG-3′	R14	5′-CAAGCTTTCCAACTCCAGTG-3′
F15	5′-GCCCTGTTTGTGCTGATACC-3′	R15	5′-CACAAGCAGAACCAGTCACC-3′
F16	5′-TGGGTTCAACTCAGCTTTGGT −3′	R16	5′-CTTTCATCATGTCATCTGCTC-3′
F17	5′-GCGAAGGAGACTCTAAGAGG-3′	R17	5′-TCTTGCTTCTTGAGATGTGGG-3′
F18	5′-CACGTATGTTATAACCATCAGC-3′	R18	5′-AGAGATAAAGGTGGAGGGCTG-3′

GGAGAAATGGCGGGTAAGGT T-3′ (forward) and 3′- GCCTCTTTACCGCCCATTCCA AGATC-5′ (reverse), respectively, where the added nucleotides for the *Nhe*I site are underlined. HEK293 or HeLa cells were cultured in growth medium supplemented with 10% fetal bovine serum, 100 IU/ml penicillin, and 100 μg/ml streptomycin at 37°C in an atmosphere of 5% CO_2. Subconfluent cells cultured in 12-well plates were transiently co-transfected with 0.5 μg pGL3-Basic vector DNA or each reporter construct (pGL3/−1993T or pGL3/−1993C) and 10 ng pRL-TK vector DNA (Promega) as an internal control for transfection efficiency, by using 1.5 μl FuGENE six transfection reagent (Roche Diagnostics, Basel, Switzerland). After 24 h, we then lysed the cells and measured firefly and *Renilla* luciferase activities in a luminometer by using the Dual-Luciferase Reporter Assay System (Promega).

Electrophoretic mobility shift assay

Nuclear extracts were prepared from HEK293 and HeLa cells as described previously (Dignam et al. 1983). Double-stranded oligonucleotides −1993T and −1993C were obtained by annealing three concatenated copies of 5′-GAAATGGTGGGTAAG-3′ and 5′-GAAATGGCGGGTAAG-3′ with their respective complementary oligonucleotides. Electrophoretic mobility shift assay (EMSA) analysis was performed by using DIG gel shift kit (Roche). We prepared digoxigenin (DIG)-labeled double-stranded oligonucleotides corresponding to the sequence at position −2000 to −1986 of the *TBX21* promoter containing the −1993 polymorphism. For each binding reaction, we incubated DIG-labeled probes with nuclear extract (2–5 μg) in 1× binding buffer (20 mM HEPES, 1 mM EDTA, 10 mM $(NH_4)_2SO_4$, 1 mM dithiothreitole, 30 mM KCl), 1 μg poly (dI-dC), and 0.1 μg poly L-lysine for 30 min on ice. For competition studies, we incubated unlabeled double-stranded oligonucleotide (100-fold molar excess) during preincubation. Reaction products were separated on 6% non-denaturing polyacrylamide gels in 0.3× TBE buffer (1× TBE buffer = 0.09 M TRIS-borate, 0.002 M EDTA, pH 8.3) and visualized by chemiluminescent detection. We scanned results into an LAS-3000 CCD camera system (Fuji Photo Film, Tokyo, Japan) and quantified each band intensity by using image analysis software Image Gauge Version 2.0 (Fuji Photo Film).

Statistical analysis

We calculated allele frequencies and tested agreement with Hardy–Weinberg equilibrium by using a χ^2 goodness of fit test at each locus. We then compared differences in allele frequencies and genotype distribution of each polymorphism between case and control subjects by using a 2×2 contingency χ^2 test with one degree of freedom or Fisher exact test and calculated odds ratios (ORs) with 95% confident intervals (95% CI). For multiple comparisons, *P*-values were corrected by the Bonferroni method. The linkage disequilibrium (LD) statistic *D′* was calculated by using the SNP Alyze statistical package (Dynacom, Chiba, Japan) as described elsewhere (Nakajima et al. 2002). Comparisons in reporter assays and EMSA experiments were performed with the Student's *t* test. A *P*-value of less than 0.05 was considered statistically significant.

Results

Screening for common polymorphisms in TBX21

Direct DNA sequencing of the indicated regions in 12 asthmatic and 12 healthy subjects (total 24 subjects) identified 24 biallelic SNPs in *TBX21*: three in the 5′ flanking region, three in the coding region (one non-synonymous and two synonymous), three in the 3′ untranslated region, and 15 in the intron (Table 2, Fig. 1). Five of these 24 SNPs (532G → C, 729G → T, 2839G → A, 9408C → A, and 10143C → A) are novel, and another 14 have been reported recently in Korean (Chung et al. 2003) and Finnish (Ylikoski et al. 2004) populations. Nucleotide position one (+1) is the first adenine of the initiation codon (ATG), and the positions for other SNPs are relative to the ATG on genome contig AC003665. A graphical overview of 24 SNPs identified in relation to the exon/intron structure of the human *TBX21* gene is given in Fig. 1. Since most of the SNPs were of relatively low frequency and in view of their location and LD with other sites, further genotyping and association studies in our asthma population focused on four SNPs: −1993T → C, 99C → G, 1298T → C, and 7725T → C. The distributions of all four SNPs were in Hardy–Weinberg equilibrium in the control group ($P > 0.05$). We calculated both *D′* and r^2 as statistical values for LD pair-wise between each SNP (Fig. 2). One of the three promoter SNPs (−1993T → C) and one synonymous coding SNP (390A → G, G130G) in exon one, were shown to be in strong LD.

TBX21 genotyping and association studies in asthma and related phenotypes

Initially, the association study was carried out on four clinical groups: child patients with asthma ($n = 361$), adult patients with atopic asthma ($n = 313$), adult patients with non-atopic asthma ($n = 88$), and adult patients with AIA ($n = 72$). Adult asthmatics, except AIA patients, had a negative reaction to the aspirin challenge or no past history of aspirin hypersensitivity. Allele frequencies of each selected SNP were compared between the patients and the normal controls by using a χ^2 test with 1 d.f. (Table 3). After correction for the number of SNPs investigated (Bonferroni correction), we found a significant association between the promoter SNP at −1993 and AIA in our Japanese cohort ($P = 0.004$;

Table 2 Locations and allele frequencies of *TBX21* SNPs in Japanese (*UTR* untranslated region)

Number	SNP	Location	Amino acid substitution	Minor allele frequency (%)	Primers
1	−1993T → C[a]	Promoter	–	8.3	F3R3
2	−1514T → C	Promoter	–	7.1	F4R4
3	− 1499G → A	Promoter	–	2.4	F4R4
4	99C → G[a]	Exon 1	H33Q	6.3	F6R6
5	390A → G	Exon 1	GI30G	8.3	F6R6
6	532G → C	Intron 1	–	2.2	F7R7
7	729G → T	Intron 1	–	4.2	F7R7
8	1298T → C[a]	Intron 1	–	16.7	F8R8
9	1662C → A	Intron 1	–	2.1	F8R8
10	2608G → A	Intron 1	–	2.1	F9R9
11	2839G → A	Intron 1	–	4.2	F9R9
12	7725T → C[a]	Intron 1	–	18.8	F11R11
13	8381A → T	Intron 1	–	16.7	F12R12
14	8762G → C	Intron 1	–	4.2	F12R12
15	9408C → A	Intron 2	–	2.3	F13R13
16	9882C → T	Intron 3	–	4.2	F14R14
17	9898C → T	Intron 3	–	4.2	F14R14
18	10143C → A	Intron 3	–	2.1	F14R14
19	10150T → C	Intron 3	–	4.2	F14R14
20	11268C → T	Intron 5	–	4.2	F16R16
21	11755G → A	Exon 6	P485P	2.1	F16R16
22	12077T → C	3′UTR	–	4.2	F17R17
23	12211G → A	3′UTR	–	2.1	F17R17
24	12403A → C	3′UTR	–	4.2	F17R17

[a]These SNPs were genotyped in a larger population

corrected P, $P_c = 0.016$). There was an increased risk for AIA associated with a C allele (OR = 1.93; 95% CI 1.22–3.06). Association analysis also demonstrated that a significant difference in allele frequency of −1993 SNP between AIA and other adult asthmatics who had no past history of aspirin hypersensitivity ($P = 0.001$). No other statistically significant association between disease status and genotype or any specific allele was detected from any of the other three case-control disease-association comparisons. We further analyzed the genotype and allele frequencies of the SNP at position 390, which was found to be in LD with SNP at −1993, in the AIA and control groups and then calculated the LD coefficient D' and r^2 between the −1993T → C and 390A → G SNPs ($D' = 0.92$; $r^2 = 0.85$). ORs of developing AIA at −1993T → C and 390A → G were 2.15 (95% CI 1.26–3.64) and 2.19 (95% CI 1.27–3.77), respectively, when the TC and TT (AG and GG) genotypes were compared with the wild-type TT (AA) genotype (Table 4). To determine whether these two SNPs in *TBX21* could also be associated with another AIA-related phenotype, we analyzed −1993T → C and 390A → G SNPs in 42 samples from independent adult AS/NP who either had a negative reaction to the aspirin challenge or no past history of aspirin hypersensitivity. Interestingly, comparison of the genotype and allele frequencies also revealed significant differences between the AS/NP group and the normal control group ($P = 0.008$ and 0.012, respectively). Furthermore, in the AIA case group, the C-allele frequency in AIA patients with NP tended to be much higher than that in AIA patients without NP (data not shown). Thus, although the sample size was small, we confirmed the *TBX21* SNP effect by using independent samples of AS/NP, regardless of aspirin hypersensitivity. We further analyzed two-loci haplotype distributions constituting the −1993T → C and 390A → G SNPs in the control, AIA, and AS/NP samples. Haplotype −1993T-390A was the

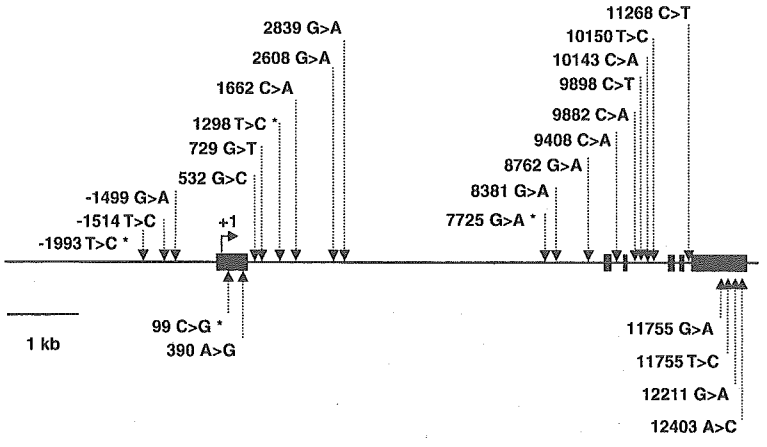

Fig. 1 Graphical overview of 24 SNPs identified in relation to the exon/intron structure of the human *TBX21* gene (*black boxes* five coding exons, *asterisks* SNPs genotyped in a larger population). Positions for SNPs are relative to the translation start site (+1)

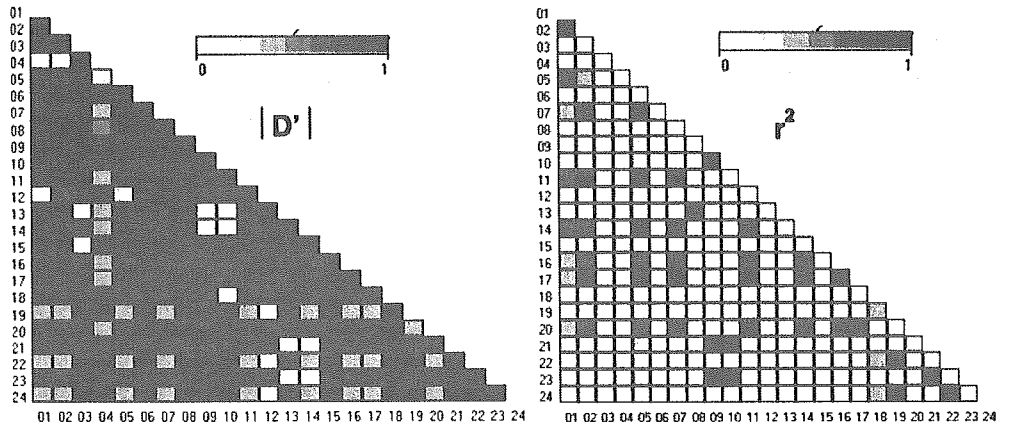

Fig. 2 Pair-wise linkage disequilibrium (*LD*) was measured by $|D'|$ and r^2 among the all of the SNPs identified in 24 sequenced samples. The blocks are *shaded* corresponding to the values obtained from the LD analysis program, SNP Alyze

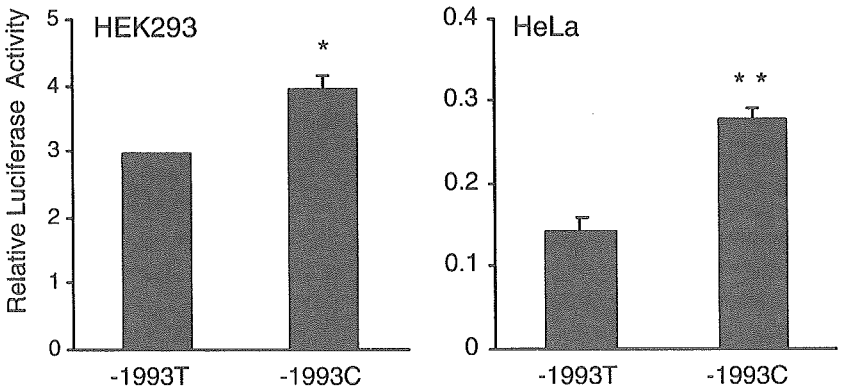

Fig. 3 Effect of the −1993T → C SNP on the transcription activity of the human *TBX21* promoter. HEK293 cells or HeLa cells were transiently cotransfected with pGL/−1993T or pGL/−1993C and pRL-TK vector. The relative luciferase activity of the *TBX21* reporter constructs is represented as the ratio of the firefly luciferase activity to that of *Renilla*. Each experiment was conducted in triplicate for each sample, and the results are expressed as mean ± SD for three independent experiments. $*P < 0.001$; $**P < 0.005$, as determined by the Student's *t* test

most common, followed by −1993C-390G and −1993C-390A. The two major haplotypes −1993T-390A and −1993C-390G were named haplotypes 1 and 2, respectively. The overall distribution of two loci haplotypes was not different between cases and controls (3 d.f.; $P = 0.10$ for AIA, and $P = 0.09$ for AS/NP), although the frequencies of two major haplotypes, haplotypes 1 and 2, were significantly different in a χ^2 test (1 d.f.; $P = 0.014$ for AIA, and $P = 0.016$ for AS/NP) (Table 4).

Transcriptional effect of TBX21 −1993T → C polymorphism

In functional assays, since the 390A → G polymorphism is a synonymous substitution, which is less likely to be directly associated with disease in general, we focused on the promoter SNP at position −1993, viz., −1993T → C. To understand the role of the T/C polymorphism at −1993 in the transcriptional regulation of the human *TBX21* gene, we performed transient expression of the −1993T and −1993C luciferase reporter constructs, pGL3/−1993T and pGL3/−1993C, in HEK293 and HeLa cells. Luciferase activity in cell extracts was analyzed after 24 h of transfection and was standardized against the internal control (*Renilla* activity). The results of this experiment showed that the −1993C construct had significantly higher luciferase reporter activity compared with the wild-type −1993T construct (33%–98% increase; $P < 0.005$). These results suggest that the −1993C allele may be associated with the increased transcriptional activity of the *TBX21* gene in human lungs.

EMSA analysis

To examine whether −1993T → C affected interaction of a nuclear factor(s) with the *TBX21* sequence around −1993, we then performed EMSAs. We prepared 2000/−1986 double-stranded oligonucleotide probes containing either the T or the C allele at −1993 bp. HEK293 nuclear extract contained nuclear proteins binding specifically to this region of the *TBX21* promoter, resulting in the formation of one major and one minor complex. Competition with 100-fold to 200-fold excess of unlabeled −1993T of −1993C probes resulted in complete inhibition of complex formation. The single band corresponding to the −1993C allele was significantly more intense than that corresponding to the −1993T allele (21% increase; $P = 0.02$ by Student's *t* test), suggesting the two different alleles had different affinities for a

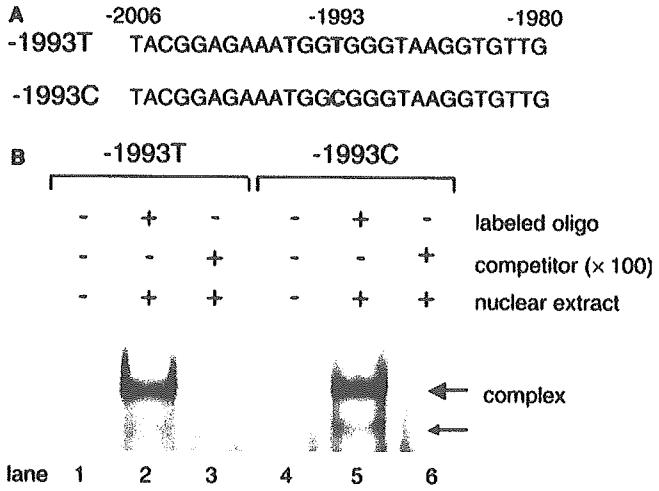

Fig. 4 EMSAs with nuclear extracts prepared from HEK293 cells. Extracts were incubated with DIG-labeled 27-bp double-stranded oligonucleotides corresponding to the −1993T or −1993C alleles of *TBX21*. Competition studies were performed by preincubating with a 100-fold excess of the unlabeled −1993T or −1993C double-stranded competitor oligonucleotides. **a** Oligonucleotide sequences containing T or C at −1993 bp (*bold*) and that were used as a probe or a competitor are shown. **b** Unknown nuclear protein of HEK293 nuclear extracts formed a much stronger complex with the −1993C oligonucleotide compared with the −1993T oligonucleotide (compare *lane 2* vs. *lane 5*; $P = 0.02$ by Student's *t* test). Binding complex was specifically competed by excess of unlabeled −1993T or C oligonucleotide (*lanes 3, 6*). Band intensity was quantified by using the LAS-3000 camera system and image analysis software Multi Gauge Version 2.0 (Fuji Photo Film). A representative result of three independent experiments is shown

particular nuclear factor. The same trend was also observed in HeLa cells (data not shown). Computer analysis of sequences covering −1993 bp, by using NSITE, available at http://www.softberry.com/berry.phtml?topic=nsite&group=programs&subgroup=promoter, indicated that the −1993T → C SNP is situated on a putative binding site for the E2F-1 transcription factor. To identify whether these putative consensus sites were involved in the transcriptional regulation of the *TBX21* gene, we performed a gel shift assay in the presence of specific anti-E2F-1 antibody (C-20; Santa Cruz Biotechnology, Calif., USA). However, preincubation with anti-E2F-1 antibody did not result in a supershift of the DNA-protein complexes (data not shown), suggesting that this protein (family) was not present in the complex binding to this region under these conditions. Together, these data indicate that the −1993T → C SNP in the human *TBX21* gene increases the affinity of an unknown nuclear protein to the binding site around −1993, leading to increased transcriptional activity and a higher expression of the T-bet protein.

Discussion

In the adaptive immune system, $CD4^+$ Th cells differentiate into at least two classes of effector cells, Th1 and Th2, in response to different pathogen-derived antigens. Th1 cells mediate cellular immunity and provide protection against intracellular pathogens and viruses, whereas Th2 cells produce IL-4, IL-5, and IL-13 and eradicate helminthes and other extracellular parasites (Mosmann and Coffman 1989). T-bet, a T box expressed in T cells, has recently been described as a master transcriptional regulator specific to IFN-γ-expressing lineages and is sufficient to induce IFN-γ and IL-12 receptor β2 expression, even under Th2-polarizing conditions (Afkarian et al. 2002; Szabo et al. 2000). Recent experiments have found that, without any allergic sensitization or challenge, the bronchi in mice lacking the T-bet gene, *tbx21*, are infiltrated with eosinophils and lymphocytes and exhibit signs of the airway remodeling and AHR to methacholine that are typical of allergic asthma (Finotto et al. 2002).

In order to examine whether polymorphisms in the candidate gene *TBX21* are related to the risk of human asthma phenotypes, we have characterized sites of

Table 3 Allele frequencies of *TBX21* SNPs in Japanese patients from different asthma groups and controls. Values are the number (%) of successfully genotyped chromosomes

Allele	Healthy controls ($n=640$)	Child patients with asthma ($n=361$)	P^a	Adult patients with					
				Atopic asthma ($n=313$)	P^a	Non-atopic asthma ($n=88$)	P^a	AIA ($n=72$)	P^a
−1993T → C									
T	1149 (89.8)	624 (89.1)		565 (90.3)		161 (93.6)		118 (81.9)	
C	131 (10.2)	76 (10.9)	0.67	61 (9.7)	0.74	11 (6.4)	0.11	26 (18.1)	0.004[b]
99C → G									
C	1127 (88.5)	617 (88.6)		509 (85.1)		143 (88.3)		116 (85.3)	
G	147 (11.5)	79 (11.4)	0.9	89 (14.9)	0.04	19 (11.7)	0.94	20. (14.7)	0.28
1298T → C									
T	1073 (83.8)	603 (83.5)		541 (87.0)		149 (84.7)		125 (86.8)	
C	207 (16.2)	119 (16.5)	0.86	81 (13.0)	0.07	27 (15.3)	0.78	19 (13.2)	0.35
7725G → A									
G	1062 (83.4)	577 (79.9)		502 (82.6)		139 (81.8)		122 (84.7)	
A	212 (16.6)	145 (20.1)	0.05	106 (17.4)	0.67	31 (18.2)	0.6	22 (15.3)	0.68

[a] *P*-value for the comparison with controls
[b] *P*-value statistically significant after Bonferroni correction (corrected $P=0.016$)

Table 4 Genotype, allele, and haplotype frequencies in Japanese AIA, AS/NP cases, and controls for the *TBX21* SNPs at—1993 and 390

Locus	Haplotype number		Controls ($n=640$)	AIA ($n=72$)	Uncorrected *P*	Odds ratio (95% CI)	AS/NP ($n=42$)	Uncorrected *P*	Odds ratio (95%)
−1993T → C		Genotype TT	519 (81.1)	48 (66.7)		1.0	27 (64.3)		1.0
		Genotype TC+CC	121 (18.9)	24 (33.3)	0.004	2.15 (1.26–3.64)	15 (35.7)	0.008	2.38(1.23–4.62)
		Allele T	1149 (89.8)	118 (81.9)		1.0	68 (81.0)		1.0
		Allele C	131 (10.2)	26 (18.1)	0.004	1.93 (1.22–3.06)	16 (19.0)	0.012	2.06(1.16–3.66)
390A → G		Genotpye AA	533 (83.3)	50 (69.4)		1.0	29 (69.0)		1.0
		Genotype AG+GG	107 (16.7)	22 (30.6)	0.004	2.19 (1.27–3.77)	13 (31.0)	0.019	2.23(1.12–4.44)
		Allele A	1165 (91.0)	120 (83.3)		1.0	70 (83.3)		1.0
		Allele G	116 (9.0)	24 (16.7)	0.004	2.01 (1.25–3.24)	14 (16.7)	0.021	2.01 (1.10–3.68)
[−1993]-[390]	1	T-A	1148 (89.7)	120 (83.3)			68 (80.9)		
	2	C-G	114 (8.9)	22 (15.3)	0.014[a]		14 (16.7)	0.016[a]	
	3	C-A	17 (1.3)	2 (1.4)			2 (2.4)		
	4	T-G	1 (0.1)	0 (0.0)	0.10[b]		0 (0.0)	0.09[b]	

[a] *P*-value for the comparison of the frequencies of haplotype 1 and 2
[b] *P*-value for the overall distribution of two loci haplotypes

genetic variation in selected genomic regions of *TBX21*. Among 24 SNPs identified (five are novel), four polymorphic sites were selected for further analysis. All SNPs fulfilled Hardy–Weinberg expectations in both asthmatic and non-asthmatic subjects, and our study showed a significant association between AIA and a SNP in the regulatory region −1993T → C of the human *TBX21* gene ($P_c=0.016$); this was found to be in strong LD with a synonymous coding SNP, 390A → G, located in exon 1 ($D'=0.92$; $r^2=0.85$). Consistent with recent data (Chung et al. 2003; Ylikoski et al. 2004), these four *TBX21* SNPs lack association with any other asthma phenotype in Japanese subjects.

The percent of the −1993C or 390G allele was much higher in AIA patients than normal controls. In an attempt to extend and support these findings, we further genotyped the −1993T → C and 390A → G SNPs in independent adult AS/NP patients and also found a significant association between these SNPs and AS/NP for the allele and genotype frequencies ($P=0.008$). Furthermore, our data indicated that the single base substitution corresponding to the −1993 *TBX21* polymorphic site produced differences in the transcriptional activity of the *TBX21* gene. Unexpectedly, the *TBX21*/−1993C reporter construct was transcriptionally more active than the wild-type −1993T construct in HEK293 and HeLa cells. In addition, EMSA analysis demonstrated that the −1993T → C substitution increased the affinity of a particular nuclear protein to the binding site of *TBX21* covering the −1993 position.

AIA refers to the development of bronchoconstriction following the ingestion of aspirin and other NSAIDs. This clinically distinct syndrome is characterized by aspirin hypersensitivity, bronchial asthma, and chronic rhinosinusitis with nasal polyposis, commonly called the "aspirin triad". AIA affects 5%–20% (about 10%) of adult asthmatics with a higher prevalence in women and is infrequently found in asthmatic children (Babu and Salvi 2000; Szczeklik and Stevenson 1999). Chronic persistent inflammation is the hallmark of patients with AIA. Recently, the importance of arachidonic acid metabolites in the pathogenesis of AIA has become apparent. The cyclo-oxygenase (COX) theory is widely accepted: AIA attacks are triggered by the specific inhibition of COX in the respiratory tract, which is followed by a reduction of prostaglandin E2 (a brake on leukotriene synthesis) and an overproduction of cysteinyl leukotrienes. Thus, cysteinyl leukotrienes have been recognized as the key mediators of AIA, but the precise molecular mechanism involved in AIA remains unclear.

Surprisingly, our results have shown a significant increase in the −1993C allele, the putative higher expression of T-bet, among patients with AIA or AS/NP, compared with controls in our Japanese cohort. An inappropriate or excess Th2-biased immune response to environmental antigens has generally been considered to play a crucial role in the development of asthma. Whereas Th2 cells promote asthmatic inflammation, Th1 cells, which secret IFN-γ, have been proposed to protect against asthma by dampening the Th2 response. However, the evidence from many studies of asthma in human and animal models conflicts with this interpretation (Busse and Lemanske 2001; Salvi et al. 2001). For example, IFN-γ production is elevated in the serum of patients with asthma (Corrigan and Kay 1990), in supernatants of bronchoalveolar lavage (BAL) cells (Cembrzynska-Nowak et al. 1993), in T cells themselves in BAL (Krug et al. 1996), and in whole blood culture (Magnan et al. 2000). By using an adaptive transfer system in mice, previous reports have shown that antigen-specific Th1 cells cause considerable airway inflammation instead of attenuating Th2-mediated lung disease (Hansen et al. 1999; Li et al. 1998; Randolph et al. 1999). IFN-γ has been demonstrated to activate eosinophils in vitro, not only with an increased expression of Fcγ receptors, CD69, HLA-DR, and intercellular adhesion

molecule-1, but also with increased viability (Busse and Lemanske 2001; Krug et al. 1996). Furthermore, therapy with IL-12, a Th1-inducing cytokine, fails to reduce AHR or the late asthmatic reaction (Bryan et al. 2000). These and other recent data (Ford et al. 2001; Sugimoto et al. 2004) suggest that IFN-γ contributes to the augmentation of allergic lung inflammation partly through the activation of eosinophils, highlighting the importance of both Th1 and Th2 cytokines in the development of asthma. Thus, the classification of allergic inflammation in asthma as a Th2-mediated disease is too simplistic (Busse and Lemanske 2001), and, as pointed out by recent work (Sugimoto et al. 2004), we propose that asthma may be classified roughly into at least two subgroups, Th2-type asthma and Th1/Th2 mixed-type asthma, including AIA.

Previous reports have suggested that Th1 cells can actually cooperate with Th2 cells in vivo and enhance Th2, eosinophil, and neutrophil recruitment by increasing the expression of TNF-α, chemokines, and adhesion molecules such as vascular cell adhesion molecule-1 (VCAM-1) in the lungs (Randolph et al. 1999; Takaoka et al. 2001). Actually, aspirin sensitivity and AS/NP often coexist with severe asthma, and the airways of AIA patients with NP show signs of persistent inflammation with marked eosinophilia and enhanced VCAM-1 expression (Hamilos et al. 1996). The continuous airway inflammation in AIA could result from a non-IgE-mediated reaction to specific endogenous or exogenous antigens such as a virus (Szczeklik 1988; Szczeklik and Stevenson 1999). A latent or chronic viral infection has been shown to alter the expression of many cellular genes, including several constituents of the arachidonic acid pathway (Zhu et al. 1998), and virally infected cells are more prone to drug and drug-metabolite-related toxicity (Levy 1997; Nakagawa et al. 2001). Moreover, an antiviral drug, acyclovir, is reported to inhibit analgesic-induced bronchoconstriction and decrease the urinary levels of leukotrieneE4 in patients with AIA (Yoshida et al. 1998). Based upon these observations of AIA, virus-specific Th1 cells responding to a respiratory tract infection could alter the local lung environment sufficiently to increase Th2 and eosinophil recruitment, leading to strong Th2 responses to inhaled antigens induced by IL-4, 5, 13, and other mediators. We postulate that the $-1993T \rightarrow C$ SNP in the *TBX21* promoter causes a functional difference in T-bet expression, resulting in increased T-bet production and (viral-induced) an excessive Th1 inflammatory reaction in the lungs.

Asthma is a phenotypically heterogeneous disorder with many etiologic factors and clinical characteristics. Although we find no associations of *TBX21* SNPs with other asthma groups except for AIA, our data also indicate that the presence of the $-1993C$ allele increases the risk of AS/NP, regardless of aspirin sensitivity. Thus, in asthma phenotypes, the *TBX21* SNPs are probably not strictly associated with aspirin sensitivity itself. NP is a chronic inflammatory disease of the paranasal sinus mucosa, leading to the protrusion of edematous polyps into the nasal cavities (Mygind 1990). NP is commonly found in association with non-atopic asthma and aspirin sensitivity, and this association of NP with asthma might reflect the shared pathophysiology of these disorders of the upper and lower airways, respectively. Furthermore, previous studies have shown that NP-infiltrating T cells expressed a mixed Th1/Th2 pattern of cytokines (Hamilos et al. 1995; Sanchez-Segura et al. 1998). Together, our present data suggested that, in a variety of asthma-related conditions, the amplification of either side of the Th1/Th2 pathway, or both, could be adverse to the host. Churg-Strauss syndrome (CSS), also known as allergic granulomatosis and angiitis, is another asthma-related disorder characterized by systemic small vessel vasculitis. Indeed, analysis of the cytokine profile of T cell lines from patients with CSS has shown both type-1 cytokine and type-2 cytokine responses (Kiene et al. 2001). Of note, clinical signs of autoimmunity such as vasculitis have been observed in some patients with AIA (Szczeklik et al. 1995, 1997).

The human *TBX21* gene is located on chromosome 17q21.32, which has previously been linked with asthma and skin tests (Dizier et al. 2000). Moreover, the region on mouse chromosome 11, a region that has been linked to AHR, is syntenically homologous to human chromosome 17q12-q22 (Zhang et al. 1999). *TBX21* is likely to be a novel candidate gene in this region, in addition to other candidate genes such as eotaxin (*CCL11*). However, our data cannot exclude the possibility that $-1993T \rightarrow C$ is in LD with another polymorphism in *TBX21* or a neighboring gene. Further studies in larger or other populations will be required to confirm the effect of the *TBX21* polymorphism. To date, several candidate genes of the enzymes in the arachidonic pathway, such as *LTC4S* and *ALOX5*, have been proposed to increase the susceptibility to AIA (Choi et al. 2004; Kawagishi et al. 2002; Sanak et al. 1997); indeed many other genes, in addition to *TBX21*, probably contribute to the pathogenesis of AIA. Genetic epidemiology on larger numbers of AIA patients is an important future requirement in order to clarify the importance of our findings.

In conclusion, we have identified 24 SNPs (five novel) in the *TBX21* gene, and our studies demonstrate that the $-1993T \rightarrow C$ SNP in the *TBX21* promoter is likely to be associated with an increased risk for AIA in Japanese. This is the first report demonstrating a relationship between the *TBX21* SNPs and clinical features of human asthma. Furthermore, we have shown that the $-1993T \rightarrow C$ polymorphism affects the transcriptional activity of the gene and may contribute to an increase in T-bet expression. In certain asthma subgroups, such as AIA and AS/NP, this promoter SNP may cause inappropriate Th1 responses in the airway, leading to severe airway inflammation, in combination with antigen-specific Th2 responses. Our present data shed light on an important area of further study regarding the precise phenotype classification of asthma by using genotypes and also focus on the Th1 response in the pathogenesis of AIA.

Acknowledgements This work was supported by grants-in-aid from the Ministry of Health, Labor, and Welfare, the Japan Science and Technology Corporation, and the Japanese Millennium project. We thank all participants in the study. We also thank Hiroshi Sekiguchi and Miki Kokubo for technical assistance and Chinatsu Fukushima for providing data on the patients.

References

Afkarian M, Sedy JR, Yang J, Jacobson NG, Cereb N, Yang SY, Murphy TL, Murphy KM (2002) T-bet is a STAT1-induced regulator of IL-12R expression in naive CD4+ T cells. Nat Immunol 3:549–557

Babu KS, Salvi SS (2000) Aspirin and asthma. Chest 118:1470–1476

Bach JF (2002) The effect of infections on susceptibility to autoimmune and allergic diseases. N Engl J Med 347:911–920

Bryan SA, O'Connor BJ, Matti S, Leckie MJ, Kanabar V, Khan J, Warrington SJ, Renzetti L, Rames A, Bock JA, Boyce MJ, Hansel TT, Holgate ST, Barnes PJ (2000) Effects of recombinant human interleukin-12 on eosinophils, airway hyperresponsiveness, and the late asthmatic response. Lancet 356:2149–2153

Busse WW, Lemanske RF Jr (2001) Asthma. N Engl J Med 344:350–362

Cembrzynska-Nowak M, Szklarz E, Inglot AD, Teodorczyk-Injeyan JA (1993) Elevated release of tumor necrosis factor-alpha and interferon-gamma by bronchoalveolar leukocytes from patients with bronchial asthma. Am Rev Respir Dis 147:291–295

Choi JH, Park HS, Oh HB, Lee JH, Suh YJ, Park CS, Shin HD (2004) Leukotriene-related gene polymorphisms in ASA-intolerant asthma: an association with a haplotype of 5-lipoxygenase. Hum Genet 114:337–344

Chung HT, Kim LH, Park BL, Lee JH, Park HS, Choi BW, Hong SJ, Chae SC, Kim JJ, Park CS, Shin HD (2003) Association analysis of novel TBX21 variants with asthma phenotypes. Hum Mutat 22:257

Cookson W (1999) The alliance of genes and environment in asthma and allergy. Nature 402:B5–B11

Corrigan CJ, Kay AB (1990) CD4 T-lymphocyte activation in acute severe asthma. Relationship to disease severity and atopic status. Am Rev Respir Dis 141:970–977

Dignam JD, Lebovitz RM, Roeder RG (1983) Accurate transcription initiation by RNA polymerase II in a soluble extract from isolated mammalian nuclei. Nucleic Acids Res 11:1475–1489

Dizier MH, Besse-Schmittler C, Guilloud-Bataille M, Annesi-Maesano I, Boussaha M, Bousquet J, Charpin D, Degioanni A, Gormand F, Grimfeld A, Hochez J, Hyne G, Lockhart A, Luillier-Lacombe M, Matran R, Meunier F, Neukirch F, Pacheco Y, Parent V, Paty E, Pin I, Pison C, Scheinmann P, Thobie N, Vervloet D, Kauffmann F, Feingold J, Lathrop M, Demenais F (2000) Genome screen for asthma and related phenotypes in the French EGEA study. Am J Respir Crit Care Med 162:1812–1818

Fahy JV, Corry DB, Boushey HA (2000) Airway inflammation and remodeling in asthma. Curr Opin Pulm Med 6:15–20

Finotto S, Neurath MF, Glickman JN, Qin S, Lehr HA, Green FH, Ackerman K, Haley K, Galle PR, Szabo SJ, Drazen JM, De Sanctis GT, Glimcher LH (2002) Development of spontaneous airway changes consistent with human asthma in mice lacking T-bet. Science 295:336–338

Ford JG, Rennick D, Donaldson DD, Venkayya R, McArthur C, Hansell E, Kurup VP, Warnock M, Grunig G (2001) Il-13 and IFN-gamma: interactions in lung inflammation. J Immunol 167:1769–1777

Hamilos DL, Leung DY, Wood R, Cunningham L, Bean DK, Yasruel Z, Schotman E, Hamid Q (1995) Evidence for distinct cytokine expression in allergic versus non-allergic chronic sinusitis. J Allergy Clin Immunol 96:537–544

Hamilos DL, Leung DY, Wood R, Bean DK, Song YL, Schotman E, Hamid Q (1996) Eosinophil infiltration in nonallergic chronic hyperplastic sinusitis with nasal polyposis (CHS/NP) is associated with endothelial VCAM-1 upregulation and expression of TNF-alpha. Am J Respir Cell Mol Biol 15:443–450

Hansen G, Berry G, DeKruyff RH, Umetsu DT (1999) Allergen-specific Th1 cells fail to counterbalance Th2 cell-induced airway hyperreactivity but cause severe airway inflammation. J Clin Invest 103:175–183

Kawagishi Y, Mita H, Taniguchi M, Maruyama M, Oosaki R, Higashi N, Kashii T, Kobayashi M, Akiyama K (2002) Leukotriene C4 synthase promoter polymorphism in Japanese patients with aspirin-induced asthma. J Allergy Clin Immunol 109:936–942

Kiene M, Csernok E, Muller A, Metzler C, Trabandt A, Gross WL (2001) Elevated interleukin-4 and interleukin-13 production by T cell lines from patients with Churg-Strauss syndrome. Arthritis Rheum 44:469–473

Krug N, Madden J, Redington AE, Lackie P, Djukanovic R, Schauer U, Holgate ST, Frew AJ, Howarth PH (1996) T-cell cytokine profile evaluated at the single cell level in BAL and blood in allergic asthma. Am J Respir Cell Mol Biol 14:319–326

Levy M (1997) Role of viral infections in the induction of adverse drug reactions. Drug Saf 16:1–8

Li L, Xia Y, Nguyen A, Feng L, Lo D (1998) Th2-induced eotaxin expression and eosinophilia coexist with Th1 responses at the effector stage of lung inflammation. J Immunol 161:3128–3135

Magnan AO, Mely LG, Camilla CA, Badier MM, Montero-Julian FA, Guillot CM, Casano BB, Prato SJ, Fert V, Bongrand P, Vervloet D (2000) Assessment of the Th1/Th2 paradigm in whole blood in atopy and asthma. Increased IFN-gamma-producing CD8(+) T cells in asthma. Am J Respir Crit Care Med 161:1790–1796

Mao XQ, Shirakawa T, Yoshikawa T, Yoshikawa K, Kawai M, Sasaki S, Enomoto T, Hashimoto T, Furuyama J, Hopkin JM, Morimoto K (1996) Association between genetic variants of mast-cell chymase and eczema. Lancet 348:581–583

Mita H, Endoh S, Kudoh M, Kawagishi Y, Kobayashi M, Taniguchi M, Akiyama K (2001) Possible involvement of mast-cell activation in aspirin provocation of aspirin-induced asthma. Allergy 56:1061–1067

Mosmann TR, Coffman RL (1989) TH1 and TH2 cells: different patterns of lymphokine secretion lead to different functional properties. Annu Rev Immunol 7:145–173

Mygind N (1990) Nasal polyposis. J Allergy Clin Immunol 86:827–829

Nakagawa H, Yoshida S, Nakabayashi M, Akahori K, Shoji T, Hasegawa H, Amayasu H (2001) Possible relevance of virus infection for development of analgesic idiosyncrasy. Respiration 68:422–424

Nakajima T, Jorde LB, Ishigami T, Umemura S, Emi M, Lalouel JM, Inoue I (2002) Nucleotide diversity and haplotype structure of the human angiotensinogen gene in two populations. Am J Hum Genet 70:108–123

Ohnishi Y, Tanaka T, Ozaki K, Yamada R, Suzuki H, Nakamura Y (2001) A high-throughput SNP typing system for genome-wide association studies. J Hum Genet 46:471–477

Randolph DA, Stephens R, Carruthers CJ, Chaplin DD (1999) Cooperation between Th1 and Th2 cells in a murine model of eosinophilic airway inflammation. J Clin Invest 104:1021–1029

Renauld JC (2001) New insights into the role of cytokines in asthma. J Clin Pathol 54:577–589

Salvi SS, Babu KS, Holgate ST (2001) Is asthma really due to a polarized T cell response toward a helper T cell type 2 phenotype? Am J Respir Crit Care Med 164:1343–1346

Sanak M, Simon HU, Szczeklik A (1997) Leukotriene C4 synthase promoter polymorphism and risk of aspirin-induced asthma. Lancet 350:1599–1600

Sanchez-Segura A, Brieva JA, Rodriguez C (1998) T lymphocytes that infiltrate nasal polyps have a specialized phenotype and produce a mixed TH1/TH2 pattern of cytokines. J Allergy Clin Immunol 102:953–960